Modelling and Simulation of 2-Dimensional Maxwell Nanofluid Using Cattaneo Christov Heat Flux Model

Kiran Mushtaq

(Fall 2016-MS CSE-9 00000172507)

A dissertation submitted in partial fulfillment of the requirements for

Master

in

Computational Science and Engineering

Supervised by

Dr. Junaid Ahmad Khan

Research Center for Modelling and Simulation

National University of Sciences and Technology

Sector H-12, Islamabad, Pakistan

February 2020

Modelling and Simulation of two dimensional Maxwell nanofluid using Cattaneo Christov heat flux model

Kiran Mushtaq

(Fall 2016-MS CSE-9 00000172507)

A dissertation submitted in partial fulfillment of the requirements for

Master

in

Computational Science and Engineering

Supervised by

Dr. Junaid Ahmad Khan

Research Center for Modelling and Simulation

National University of Sciences and Technology

Sector H-12, Islamabad, Pakistan

February 2020

Dedicated to

My Mother

(*Shamim Akhter*)

Acknowledgment

I am going to start with the thanks of ALLAH, who gave the vigor to fulfill my jobs.

Every students projects own debt to their predecessors to their teachers, their parents and family and their friends.

I gratefully acknowledge my deep indebtedness to my supervisor Dr. Junaid Ahmad khan (Assistance Professor, RCMS, NUST), for his never ending promotion, provocation, precious supervision and his valuable time throughout my work, along with him I would like to be beholden to my GEC member Dr. Adnan Maqsood (HOD Research, RCMS, NUST), Dr. Ammar Mushtaq (Assistance Professor, RCMS, NUST) and Dr. Salma Sherbaz (Assistance Professor, RCMS, NUST).

This goal was unable to achieve without the support of my parents (Mr. and Mrs. Mushtaq Ahmed), my husband (Mr. Musharraf Ahmad Khan), my kids (Emma and Haider), my father in-law (Mr. Mahmood Ahmad Khan) and my brothers.

I am also grateful to the RCMS, NUST department who supports me a lot, without their corporation it was impossible to complete my MS Program.

Kiran Mushtaq

Table of Contents

List of Abbreviations

x, y - Cartesian coordinates

u, v - Velocity component in x, y - directions

T - Temperature

t - Time

p - Fluid pressure

Pr - Prandtal number

k - Thermal conductivity

C_p - Specific heat capacity

μ - viscosity

ρ - density

Le - Lewis number

Nu - Nusselt number

h - convective heat transfer

Bi - Biot number

Sc - Schmidt number

D - mass diffusivity

τ - shear stress

q - heat flux

D_B - Brownian motion diffusion

D_T - Thermophoretic diffusion

C - Nanoparticles volume fraction

T_f - fluid temperatur

T_∞ - Ambient temperature

T_w - Wall temperature

ψ - Stream function

η - Similarity variable

a_1 - fluid relaxation parameter

a_2 - Thermal relaxation parameter

Nu_x - Local Nusselt number

C_f - Skin friction coefficient

λ_1 - fluid relaxation time

λ_2 - Thermal relaxation time

List of Tables

List of Figures

Abstract

Boundary layer flows have a vast application in various fields due to heat transfer. Now scientist and researchers are using nanofluids, which is an engineered heat transfer fluid prepared by nanometer sized particles, for enhancing the heat transfer rate. As our main work was on Maxwell materials (which are also known as Maxwell fluids) the governing equations for nanofluid were developed by combining upper convective Maxwell fluid model and Cattaneo Christov heat flux model. In order to formulate the mathematical model of nanofluid, non-homogeneous model and homogeneous model were considered. Simulations were performed on Ethanol based non-Newtonian nanofluid for 2-dimension boundary layer flow due to the linearly stretching sheet. As in non-homogeneous model heat flux is the sum of conductive heat flux and diffusive heat flux due to nanoparticles, while doing literature review it was observed that the part of diffusive heat flux is neglected in the derivation of energy equation for non-homogeneous model using Canttaneo-Christov heat flux model which is incorporated in this thesis. The numerical results were obtained using Keller-Box method and bvp4c in Matlab. Thermal relaxation parameter and fluid relaxation parameter are exhibiting the increasing behavior on thermal boundary layer profile and skin friction coefficient respectively with homogeneous model. In non-homogeneous model Prandtl number, thermal relaxation parameter and Brownian motion parameter are reducing the thickness of thermal boundary layer and concentration boundary layer. For revised Canttaneo-Christov heat flux model we have obtained unrealistic results for high values of Brownian motion parameter. The results are present in both tabular and graphically in their respective chapters and the conclusions are present at the end.

Chapter 1
Introductory Background

In this chapter we have discussed the background of the boundary layer, nanofluid, along and the basics definitions of different parameters which were used in the given exposition. Derivation of governing equations for non-Newtonian fluid is described, at the end of this chapter the solution methodology is discussed.

1.1 History

Boundary layer is a compelling part in fluid mechanics. It forms in the layer of fluid in the immediate vicinity of bounding surface. In this area the viscosity effect is very important. In 1904, a group of mathematicians and scientists gathered in Germany for third international mathematics congress. In this conference Ludwig Prandtl [1] presented the concept of boundary layer theory. Prandtl's PhD student Blasius solved first boundary layer problem to overcome the conundrum of turbulence. He solved this problem by using analytical techniques and obtains the solution in terms of series expansion. Crane [2] did the work on the extension of Blasius flow in 1970 that is boundary layer on stretching sheet. Mostly it happens in the making of plastic sheets. He focused on heat conduction in the linear stretching sheet.

1.1.1 Nanofluid

In twenty first century it has seen a marvelous development in technological industry. The concept of Nano science is based on a phrase "there's a plenty of room at the bottom" by the noble prize-winning physicist Richard Feynman in 1959. He proposed the concept of micro machines. In 1974 scientist Norio Taniguchi used the term nanotechnology. Masuda at el discovered in 1993 that both viscosity and thermal conductivity can be enhanced by dispersing nanometer-sized metallic particles in the fluid, following them in 1995 Choi and Eastman [3]

prepared nanofluid successfully in Argonne laboratory USA. After that nanofluids grab the attention of the researchers almost all over the world.

Nanofluid is a suspension which is made by non-metallic or a metallic particle in any kind of fluid such as liquid, gas etc. After having these particles this fluid has a better response of heat transfer [4].

We have two types of nanofluid. Metallic nanofluid which fluid have a metallic nanoparticles such as aluminum, copper, nickel etc, known as metallic nanofluid and nonmetallic nanofluid which fluids are having nonmetallic nanoparticles such as metal oxide, allotropes of carbon (diamond, graphite) etc.

Nanofluid has some very special qualities such as:

- Rise in thermal conductivity.
- Better stability.
- Reduction of clogging and erosion.
- Better heat transfer ability.

1.1.2 Applications of nanofluid

It has a various fields of application in engineering such as:

- Electronic cooling
- Transportation (Engine cooling/Vehicle thermal management)
- Nuclear system cooling
- Medical equipment's
- Heat exchanger
- Transformer
- Rotating machinery
- Gas turbine rotors
- Air cleaning mechanic's
- heating, Chillers Other applications (Heat pipes, Fuel cell, Solar water, Drilling, Lubrications)

1.2 Definitions

Some useful terminologies are described below:

- **Prandtl number** is a dimensionless quantity, which is defined as a ratio between the kinematic viscosity and a thermal diffusivity.

$$Pr = \frac{Kinematic\ viscosity}{Thermal\ diffusivity} = \frac{{}^{\mu}/_{\rho}}{{}^{k}/_{\rho c_p}} = \frac{\mu c_p}{k} \tag{1.1}$$

Where $k =$ thermal conductivity, $C_p =$ specific heat capacity, $\mu =$ viscosity

- **Lewis number** is a dimensionless number and describes as a ratio between the thermal diffusivity and the mass diffusivity.

$$Le = \frac{Thermal\ diffusivity}{Mass\ diffusivity} = \frac{{}^{k}/_{\rho C_p}}{D} = \frac{k}{\rho C_p D} \tag{1.2}$$

Where $k =$ thermal conductivity, $\rho =$density, $C_p =$specific heat capacity, $D =$mass diffusivity

- **Nusselt number** is used to calculate the heat transfer between a moving fluid and a solid body. It is also a dimensionless quantity and defined as

$$Nu = \frac{convective\ heat\ transfer}{conductive\ heat\ transfer} = \frac{h}{{}^{k}/_{L}} = \frac{hL}{k} \tag{1.3}$$

Where $h =$ convective heat transfer coefficient, $L =$ length, $k =$ thermal conductivity

- **Biot number** is a dimensionless quantity and is used to calculate the heat transfer at and inside the surface of solid body.

$$B_i = \frac{L_c h}{k} \tag{1.4}$$

Where $L_c = volume\ of\ body/surface\ area$, $h =$ convective heat transfer coefficient, $k =$ thermal conductivity

- **Schmidt number** is a dimensionless quantity and defined as the ration between the kinematic viscosity and mass diffusivity.

$$Sc = \frac{kinematic\ viscosity}{mass\ diffusivity} = \frac{\nu}{D} \tag{1.5}$$

- **Sherwood number** helps to calculate mass transfer and define as the ratio between convective mass transfer and a diffusion rate. It is also a dimensionless number.

$$sh = \frac{convective\ mass\ transfer}{diffusion\ rate} = \frac{h}{D/L} = \frac{hL}{D} \quad (1.6)$$

Where $h =$ convective heat transfer coefficient, $L =$ characteristics length, $D =$ mass diffusivity

Rayleigh number exhibits the instability of layer of fluid which becomes due to the density and temperature difference.

- **Brownian motion** defined as a random motion of particles (which are dispersed in a fluid) as the consequences of their collision with the other moving particles in the fluid.
- **Thermophoresis** defined as a response of a different moving particle towards the temperature gradient in a fluid.
- **Darcy model** describes the flow of fluid through the porous medium which was formulated by Henry Darcy.
- **Similarity Parameters** the dimensionless solution depends on the group of non-dimensional parameters. These parameters are known as similarity parameters.
- **Newtonian fluids** a fluid which holds the linear relationship between the shear stress and rate of change of deformation are known as Newtonian fluid. Air and water are the example of Newtonian fluids.

$$\tau = \mu \frac{du}{dy} \quad (1.7)$$

- **Non-Newtonian fluids** a fluid which holds the non-linear relationship between the shear stress and rate of change of deformation are known as non-Newtonian. Except water and air all fluids are the example of non-Newtonian fluids.

$$\tau = \mu \left(\frac{du}{dy}\right)^n \quad (1.8)$$

1.3 Literature Review

Nanofluids are formed with nanoparticles and base fluids; they are designed to have high thermal conductivity. Earlier heat transfer rate of nanofluid was calculated by traditional fluid correlations such as Dittus-Boelter's but it does not gives accurate solutions in high temperature and rough surface.

In generally nanofluid exhibits high thermal conductivity effect, this behavior is due to thermal dispersion and the reason of the intensified turbulence is the motion of nanoparticles. To check the validity of this assumption Buongiorno [5] consider the seven slip mechanisms in 2006. These mechanisms produce relative velocity between nanoparticles and base fluid. After that work we came to conclude that among these seven slip mechanisms only Brownian diffusion and Thermophoresis parameters are dominant in nanofluids. In sight of these results Buongiorno describes nanofluid with a non-homogenous equilibrium models for mass, momentum and heat transfer, so to neglect the transfer of energy which is due to dispersion of nanoparticles.

In 2008 Christov has proposed the new version of Fourier's law which is known as Cattaneo Christov heat flux model. According to Fourier law temperature raises abruptly in spite of that Christov considered some relaxation time. Tzou [6] worked in 2008 about the thermal uncertainty in nanofluids. He focuses to observe the combined behavior of Brownian motion and Thermophoresis of nanoparticles, also he observed that the critical Reyleigh number for nanofluids exhibit lower than for regular fluid. Highly promoted turbulence increases the energy y bearing capacity of nanofluids, because of this entire overall heat transfer coefficient increases rather than increase in thermal conductivity alone. The important equations are calculated by using non-dimensional parameters. In 2009 Kuznetsov and Nield [7] calculated the effect of nanofluids on natural convection boundary layer flow in a porous medium. He considered the Darcy model for momentum equation with simplest boundary conditions. He calculated the Nusselt number Nu by using the Brownian motion Nb, Lewis number Le, Thermophoresis parameter Nt, Buoyancy-ratio parameter Nr, which depict the wall heat flux. Incompressible Newtonian fluid with gravity acting downwards was considered by Straughan [8] in 2009. For heat flux phenomena Cattaneo Christov model was taken by author.

Khan and Pop [9] exhibit first paper on stretching sheet in nanofluids in 2010. They considered a nanofluid model which is based on Brownian motion and Thermophoresis for laminar fluid flow. They calculated the reduce Sherwood number and reduced Nusselt number by using the Brownian motion and Thermophoresis parameter for different values of Prandtl number and Lewis number (Schmidt number in actuality error in paper). After their analysis we came to know that the reduce Nusselt number is a decreasing function for all dimensionless parameters instead of that for all values of Lewis number, Brownian motion and Thermophoresis, the reduce Sherwood number is an increasing function for higher Prandtl number and decreasing function for lower Prandtl number.

In 2010 Kuznetsov and Nield [10] again worked on nanofluid natural convective boundary layer flow which past a vertical plate. Now they concentrated on analytical solution. They considered a nanofluid model which includes the effect of Brownian motion and Thermophoresis parameter. The solution was depended on five different parameters. The analysis depicts for all the values of Buoyancy-ratio, Brownian motion, Thermophoresis parameter the reduced Nusselt number is a decreasing function. Cortell [11] worked on numerical comparison of Blasius and Sakiadis flow.

In 2011 Makinde and Aziz [12] focused on numerical study of the boundary layer flow of nanofluids which forms due to linearly stretching sheet. They also considered the model which incorporates the effect of Brownian motion and Thermophoresis. After the solution it was noticed that the thickness of thermal boundary layer increases with the strong effect of Brownian motion, thermophoresis. Lewis number (Schmidt number) shows a small effect on temperature distribution. For fixed Thermophoresis, Brownian motion, Prandtl number, Lewis number the concentration profile increases with the increased Biot number but as the Lewis number increases the concentration profile decreases. When the Brownian motion and Thermophoresis parameter intensify with the fixed Prandtl number, Lewis number and Biot number the reduce Nusselt number decreases and the reduce Sherwood number increases.

Hatami et al. [13] concentrated on laminar flow. He worked on boundary layer flow of nanofluids on rotating disk. For thermal conductivity Chon model and for viscosity Brinkman model considered. Fourth order Runge Kutta Fehlberg and least method was used to solved the governing equations. After the calculation it depicts that temperature increases with the increment on s. For coupled flow (a flow in which temperature gradient produce both an electric

current flow and heat flow) Shihao Han considered an upper convective Maxwell fluid with Cattaneo Christov heat flux model on stretching sheet in 2014.

In 2015 Mustafa et al. [14] worked on so called Bödewadt boundary layer flow. Bödewadt flow is rotating flow far away from the rotating disk. After applying the similarity transformation, the governing equations are highly non-linear. After the solution of the equations it is clearly seen that temperature profile is decreasing even for an ordinary strength. This result is very significant in practical application, as it shows due to this system may be cool down soon.

Abu Bakar et al. [15] worked on boundary layer of stretching sheet by using non-homogeneous model. By using the similarity parameters transformed the governing partial differential equations into non-linear ordinary differential equations. He applied the shooting method to solve these equations. After the result it is clearly seen that with the increment of φ Brownian motion and thermophoresis parameters decreases and the heat transfer rate increases. Cattaneo christov heat flux model with upper convective Maxwell fluid over a exponentially stretching surface was examined by Ahmad et al. [16].

Ali and Sandeep [17] in 2016 focused on magneto hydrodynamic casson-ferrofluid over a cone with nonlinear radiation effects and variable source/sink, Cattaneo Christov heat flux model was considered. Anticipatedly nanoparticles were moving in the base fluid but the motion of nanoparticles become uniformly after applying the magnetic field. 3-dimension Cattaneo Christov heat flux model with Maxwell fluid was examined by Munir and Shehzad [18]. In this case sheet was stretching bi-directionally. In same year rotating flow of upper convective Maxwell fluid with Cattaneo Christov heat flux model was observed by Mustafa et al. [19]. MHD 3-dimension of UCM fluid over a bi-directional stretching surface was examined by Rubab and Mustafa [20] and Cattaneo Christov heat flux model was taken by her instead of Fourier law.

MHD Maxwell fluid with Cattaneo heat flux model on non-Darcy porous medium was under consideration by Muhammad et al. [21] in 2017. Imran et al. [22] introduced a chemical reaction model with Maxwell fluid in 2017. In the same year for mass transfer MHD flow of an upper convective Maxwell fluid and for heat transfer Cattaneo Christov heat flux model over a stretching sheet was focused by Shahid et al. [23]. Thermal radiation and chemical reaction effects are also considered.

First time turbulent non-Newtonian nanofluids were investigated in 3-D micro tube by Rahimi et al. [24]. The researcher obtained the results which are fruitful for those who work on cooling system in electronic devices. Performance of non-Newtonian with TiO_2 nanoparticles and the solution of carboxymethyl cellulose in square channel was under consideration by Amani et al. [25]. Non-Newtonian nanofluids with aluminum oxide through the applications of different slip conditions was studied by Goodarzi et al. [26]. Flow and heat transfer of pseudo-plastic non-Newtonian nanofluids with suction injection was followed by Maleki and Reza [27]. He also did the comparison between the behavior of Newtonian nanofluid and non-Newtonian nanofluid. In non-Newtonian fluid nonlinear jerk equation of velocity for non-uniform oscillation was studded by Zongmin and Zhang [28]. This particular model is established by experimental data.

Casson nanofluid flow past over a swirling cylinder with Cattaneo-Christov heat flux was discussed by Alebraheem and Ramzan [29] in 2019. Sodium alginate non-Newtonian nanofluid between two vertical flat plates focused by Saadatmandi and Shateri [30]. Parand t al. [31] worked on Powell-Eyring non-Newtonian fluid over a stretching sheet. Unsteady natural convective flow of Newtonian, non-Newtonian fluid in a square closure was presented by Pishkar et al. [32]. G. Sarojamma et al. [33] considered Cattaneo-Christov heat flux model with autocatalytic chemical reaction in 2019.

1.4 General Equations

The continuity, momentum and energy equation of Newtonian, non-Newtonian fluid are given below. Let us consider an isothermal, incompressible, steady flow. Where $\boldsymbol{V}$ is the velocity vector, ρ is the density, μ is the viscosity of fluid.

1.4.1 Continuity Equation

Continuity equation of Newtonian and non-Newtonian is same and given below:

$$\boldsymbol{\nabla}.\boldsymbol{V} = 0 \tag{1.9}$$

1.4.2 Momentum Equation

Momentum equation is given as:

$$\rho(\boldsymbol{V}.\boldsymbol{\nabla})\boldsymbol{V} = \boldsymbol{\nabla}.\boldsymbol{\sigma} \tag{1.10}$$

Where $\boldsymbol{\sigma} = -pI + \boldsymbol{\tau}$, we are not considering any pressure terms $\boldsymbol{\sigma} = \boldsymbol{\tau}$. Now the above equation becomes

$$\rho(\boldsymbol{V}.\boldsymbol{\nabla})\boldsymbol{V} = \boldsymbol{\nabla}.\boldsymbol{\tau} \tag{1.11}$$

Where $\boldsymbol{\tau}$ is extra stress tensor defined as $\boldsymbol{\tau} = \mu \boldsymbol{A}_1$ where $\boldsymbol{A}_1 = \boldsymbol{\nabla V} + (\boldsymbol{\nabla V})^T$ is first Rivlin Ericksen tensor. The above is the momentum equation for Newtonian fluid. In case of Maxwell fluid the $\boldsymbol{\tau}$ is defined by the following relation

$$\left(1 + \lambda_1 \frac{D}{Dt}\right)\boldsymbol{\tau} = \mu \boldsymbol{A}_1 \tag{1.12}$$

In this equation $\lambda_1$is fluid relaxation time, $\frac{D}{Dt}$ is convective time derivative. For any vector **A** we have

$$\frac{D}{Dt}(\boldsymbol{A})_i = \frac{\partial}{\partial t}(\boldsymbol{A})_i + \boldsymbol{V}_j(\boldsymbol{A})_{i,j} - \boldsymbol{V}_{i,j}(\boldsymbol{A}_j) \tag{1.13}$$

Now applying $\boldsymbol{\nabla}$ on both sides of equation (1.12)

$$\boldsymbol{\nabla}.\left(1 + \lambda_1 \frac{D}{Dt}\right)\boldsymbol{\tau} = \boldsymbol{\nabla}.(\mu \boldsymbol{A}_1) \tag{1.14}$$

$$\left(1 + \lambda_1 \frac{D}{Dt}\right)\boldsymbol{\nabla}.\boldsymbol{\tau} = \mu \boldsymbol{\nabla}.\boldsymbol{A}_1 \tag{1.15}$$

From equation (1.11) replace the value of $\boldsymbol{\nabla}.\boldsymbol{\tau}$, so the above equation becomes,

$$\left(1 + \lambda_1 \frac{D}{Dt}\right)\rho \frac{d\boldsymbol{V}}{dt} = \mu \nabla.\boldsymbol{A}_1 \tag{1.16}$$

From equation (1.13) for i=1, j=1, 2, 3

$$\frac{D}{Dt}\left(\frac{d\boldsymbol{V}}{dt}\right)_1 = \frac{\partial}{\partial t}\left(\frac{d\boldsymbol{V}}{dt}\right)_1 + V_1\left(\frac{d\boldsymbol{V}}{dt}\right)_{1,1} + V_2\left(\frac{d\boldsymbol{V}}{dt}\right)_{1,2} - V_{1,1}\left(\frac{d\boldsymbol{V}}{dt}\right)_1 - V_{1,2}\left(\frac{d\boldsymbol{V}}{dt}\right)_2 \tag{1.17}$$

And the following terms are defined as

$$V_1 = u, \;\; V_2 = v$$

$$\begin{aligned}
\left(\frac{d\boldsymbol{V}}{dt}\right)_1 &= \frac{du}{dt} = u\frac{\partial u}{\partial x} + v\frac{\partial u}{\partial y} \\
\left(\frac{d\boldsymbol{V}}{dt}\right)_2 &= \frac{dv}{dt} = u\frac{\partial v}{\partial x} + v\frac{\partial v}{\partial y} \\
\left(\frac{d\boldsymbol{V}}{dt}\right)_{1,1} &= \frac{\partial}{\partial x}\left(u\frac{\partial u}{\partial x} + v\frac{\partial u}{\partial y}\right) \\
\left(\frac{d\boldsymbol{V}}{dt}\right)_{1,2} &= \frac{\partial}{\partial y}\left(u\frac{\partial u}{\partial x} + v\frac{\partial u}{\partial y}\right)
\end{aligned} \qquad (1.18)$$

Table 1.1 Boundary layer assumptions, the order of magnitude

Variables	Order of magnitude
u	1
$\frac{\partial}{\partial x}$	1
v	ε
$\frac{\partial}{\partial y}$	$\frac{1}{\varepsilon}$
ν	ε^2

By using all these above equations, equation (1.16) becomes for x - component

$$u\frac{\partial u}{\partial x} + v\frac{\partial u}{\partial y} + \lambda_1\left(u^2\frac{\partial^2 u}{\partial x^2} + 2uv\frac{\partial^2 u}{\partial x \partial y} + v^2\frac{\partial^2 u}{\partial y^2}\right) = \nu\left(\frac{\partial^2 u}{\partial x^2} + \frac{\partial^2 u}{\partial y^2}\right) \qquad (1.19)$$

Where ν is the kinematic viscosity, similarly the equation for y - component

$$u\frac{\partial v}{\partial x} + v\frac{\partial v}{\partial y} + \lambda_1\left(u^2\frac{\partial^2 v}{\partial x^2} + 2uv\frac{\partial^2 v}{\partial x \partial y} + v^2\frac{\partial^2 v}{\partial y^2}\right) = \nu\left(\frac{\partial^2 v}{\partial x^2} + \frac{\partial^2 v}{\partial y^2}\right) \qquad (1.20)$$

Now use the boundary layer assumption, the order of magnitude. The above equation (1.20) vanishes and equation (1.19) becomes

$$u\frac{\partial u}{\partial x}+v\frac{\partial u}{\partial y}+\lambda_1\left(u^2\frac{\partial^2 u}{\partial x^2}+2uv\frac{\partial^2 u}{\partial x\partial y}+v^2\frac{\partial^2 u}{\partial y^2}\right)=\nu\left(\frac{\partial^2 u}{\partial y^2}\right) \quad (1.21)$$

- **Momentum equation for nanofluid**

We will follow two different types of models for transportation of nanofluid.

- **Homogeneous**
- **Non-Homogeneous**

In homogeneous [34] model viscosity is $\frac{\mu_{nf}}{\rho_{nf}}$ instead of $\frac{\mu}{\rho}$, so the momentum equation becomes

$$u\frac{\partial u}{\partial x}+v\frac{\partial u}{\partial y}+\lambda_1\left(u^2\frac{\partial^2 u}{\partial x^2}+2uv\frac{\partial^2 u}{\partial x\partial y}+v^2\frac{\partial^2 u}{\partial y^2}\right)=\frac{\mu_{nf}}{\rho_{nf}}\left(\frac{\partial^2 u}{\partial y^2}\right) \quad (1.22)$$

Where density of nanofluid is ρ_{nf}, dynamic viscosity of nanofluid is μ_{nf}, they are defined as:

$$\mu_{nf}=\frac{\mu_f}{(1-\varphi)^{2.5}},$$
$$\rho_{nf}=(1-\varphi)\rho_f+\varphi\rho_{s,} \quad (1.23)$$

Where φ is the nanoparticle volume fraction, μ_f is the dynamic viscosity of base fluid, ρ_f is the density of the base fluid, ρ_s is the density of the nanoparticle material. The equation(1.21) remains same in homogeneous [35] model.

1.4.3 Energy Equation

Energy equation is given as:

$$(\rho c)_p(\boldsymbol{V}\boldsymbol{\nabla}.T)=-\boldsymbol{\nabla}.\boldsymbol{q} \quad (1.24)$$

Where $\boldsymbol{q}$ is the heat flux using Fourier law, T is the temperature and $(\rho c)_p$is specific heat capacity.

Heat flux in Cattaneo Christov heat flux model is obtained by following relationship:

$$\left(1+\lambda_2\frac{D}{Dt}\right)\boldsymbol{q}=-k\boldsymbol{\nabla}\mathrm{T} \quad (1.25)$$

- **Energy equation for nanofluid**

For transportation of nanofluid in energy equation we will follow the same models. First we will focus on homogeneous model then a detailed derivation of non-homogeneous model.

- **Homogeneous Model**

In Cattaneo Christov heat flux for homogeneous model the kinematic viscosity changes, the above equation (1.25) becomes:

$$\left(1+\lambda_2\frac{D}{Dt}\right)\boldsymbol{q}=-k_{nf}\boldsymbol{\nabla}\mathrm{T} \tag{1.26}$$

After simplifying the above equation (1.26), it becomes

$$u\frac{\partial T}{\partial x}+v\frac{\partial T}{\partial y}+\lambda_2\left[u^2\frac{\partial^2 T}{\partial x^2}+v^2\frac{\partial^2 T}{\partial y^2}+2uv\frac{\partial^2 T}{\partial x\partial y}+\left(u\frac{\partial u}{\partial x}+v\frac{\partial u}{\partial y}\right)\frac{\partial T}{\partial x}\right. \tag{1.27}$$
$$\left.+\left(u\frac{\partial v}{\partial x}+v\frac{\partial v}{\partial y}\right)\frac{\partial T}{\partial y}\right]=\alpha_{nf}\left(\frac{\partial^2 T}{\partial y^2}\right)$$

Where α_{nf} is the thermal diffusivity of nanofluid, it is defined as:

$$\alpha_{nf}=\frac{k_{nf}}{(\rho c_p)_{nf}}, \tag{1.28}$$

$$\frac{k_{nf}}{k_f}=\frac{\left(k_s+2k_f\right)-2\varphi(k_f-k_s)}{\left(k_s+2k_f\right)+\varphi(k_f-k_s)}, \tag{1.29}$$

$$(\rho c_p)_{nf}=(1-\varphi)\left(\rho c_p\right)_f+\varphi(\rho c_p)_s, \tag{1.30}$$

Where φ is the nanoparticle volume fraction, k_{nf} is the thermal conductivity of nanofluid, in which k_f is thermal conductivity of base fluid and k_s is the thermal conductivity of the nanoparticle material and $(\rho c_p)_{nf}$ is the effect of heat capacity of nanofluid, in which $\left(\rho c_p\right)_f$ is the effective heat capacity of base fluid and $\left(\rho c_p\right)_s$ is the effective heat capacity of nanoparticle material.

- **Non-Homogeneous Model**

Cattaneo Christov [36] heat flux model for non-homogeneous model in literature is given as:

$$\left(1+\lambda_2\frac{D}{Dt}\right)\boldsymbol{q}=-k\boldsymbol{\nabla}\mathrm{T} \tag{1.31}$$

$$u\frac{\partial T}{\partial x}+v\frac{\partial T}{\partial y}+\lambda_2\left[u^2\frac{\partial^2 T}{\partial x^2}+v^2\frac{\partial^2 T}{\partial y^2}+2uv\frac{\partial^2 T}{\partial x\partial y}+\left(u\frac{\partial u}{\partial x}+v\frac{\partial u}{\partial y}\right)\frac{\partial T}{\partial x}\right.$$
$$\left.+\left(u\frac{\partial v}{\partial x}+v\frac{\partial v}{\partial y}\right)\frac{\partial T}{\partial y}\right] \qquad (1.32)$$
$$=\frac{k}{(\rho c)_f}\left(\frac{\partial^2 T}{\partial y^2}\right)+\frac{(\rho c)_p}{(\rho c)_f}\left[D_B\left(\frac{\partial T}{\partial y}\frac{\partial C}{\partial y}\right)+\frac{D_T}{T_\infty}\left(\frac{\partial T}{\partial y}\right)^2\right]$$

Where λ_2 is a fluid relaxation time, $\boldsymbol{q}$ is a heat flux and defined as $\boldsymbol{q}=-k\boldsymbol{\nabla}T+h_s j_s$, k is a thermal conductivity and $h_s j_s$ shows nanoparticles term, h_s is the specific enthalpy and defined as $h_s=c_pT$, j_s is a diffusive mass flux and defined as $j_s=j_{s,B}+j_{s,T}$, $j_{s,B}$ is defined as $j_{s,B}=-\rho_s D_B\boldsymbol{\nabla}c$, in which $D_B$is a Brownian motion diffusion coefficient, $j_{s,T}$ is defined as $j_{s,T}=-\rho_s D_T\frac{\boldsymbol{\nabla}T}{T_\infty}$, in which D_T is a Thermophoretic diffusion coefficient. The above equation (1.31) is used in present literature and the derivation is already available.

While having the literature review it was notified that the part of heat flux due to nanoparticles diffusion is neglected as in equation (1.31), after including that part in the derivation of energy equation using Cattaneo-Christov heat flux model and non-homogeneous model is given below:

$$\rho C_p\left(\frac{\partial T}{\partial t}+\boldsymbol{V}.\boldsymbol{\nabla}T\right)=-\boldsymbol{\nabla}.\boldsymbol{q}+h_s\boldsymbol{\nabla}.j_s \qquad (1.33)$$

In the above equation $h_s j_s$ shows nanoparticles behavior term.

Equation (1.31) after adding diffusive heat flux term becomes

$$\left(1+\lambda_2\frac{D}{Dt}\right)\boldsymbol{q}=-k\boldsymbol{\nabla}\mathrm{T}+h_s j_s \qquad (1.34)$$

$$\left(\boldsymbol{q}+\lambda_2\left(\frac{\partial \boldsymbol{q}}{\partial t}+\boldsymbol{V}.\boldsymbol{\nabla}\boldsymbol{q}-\boldsymbol{q}.\boldsymbol{\nabla}\boldsymbol{V}+(\boldsymbol{\nabla}.\boldsymbol{V})\boldsymbol{q}\right)\right)=-k\boldsymbol{\nabla}\mathrm{T}+h_s j_s \qquad (1.35)$$

Applying $\boldsymbol{\nabla}$. On both sides of the above equation, so the above equation becomes

$$\boldsymbol{\nabla}.\left(\boldsymbol{q}+\lambda_2\left(\frac{\partial \boldsymbol{q}}{\partial t}+\boldsymbol{V}.\boldsymbol{\nabla}\boldsymbol{q}-\boldsymbol{q}.\boldsymbol{\nabla}\boldsymbol{V}+(\boldsymbol{\nabla}.\boldsymbol{V})\boldsymbol{q}\right)\right)=\boldsymbol{\nabla}.(-k\boldsymbol{\nabla}\mathrm{T}+h_s j_s) \qquad (1.36)$$

Now

$$\boldsymbol{\nabla}.\boldsymbol{q}+\lambda_2\boldsymbol{\nabla}.\left(\frac{\partial \boldsymbol{q}}{\partial t}+\boldsymbol{V}.\boldsymbol{\nabla}\boldsymbol{q}-\boldsymbol{q}.\boldsymbol{\nabla}\boldsymbol{V}+(\boldsymbol{\nabla}.\boldsymbol{V})\boldsymbol{q}\right)=-k\boldsymbol{\nabla}.\boldsymbol{\nabla}\mathrm{T}+\boldsymbol{\nabla}.(h_s j_s) \tag{1.37}$$

$$\begin{aligned}\boldsymbol{\nabla}.\boldsymbol{q}+\lambda_2\left(\boldsymbol{\nabla}.\left(\frac{\partial \boldsymbol{q}}{\partial t}\right)+\boldsymbol{\nabla}.(\boldsymbol{V}.\boldsymbol{\nabla}\boldsymbol{q})-\boldsymbol{\nabla}.(\boldsymbol{q}.\boldsymbol{\nabla}\boldsymbol{V})+\boldsymbol{\nabla}.((\boldsymbol{\nabla}.\boldsymbol{V})\boldsymbol{q})\right)\\ =-k\nabla^2\mathrm{T}+(h_s\boldsymbol{\nabla}.j_s+j_s.\boldsymbol{\nabla}h_s)\end{aligned} \tag{1.38}$$

As we have $\boldsymbol{\nabla}.(h_s j_s)=h_s\boldsymbol{\nabla}.j_s+j_s.\boldsymbol{\nabla}h_s$, as we are considering steady flow$\Longrightarrow\frac{\partial \boldsymbol{q}}{\partial t}=0$.

$$\begin{aligned}\boldsymbol{\nabla}.\boldsymbol{q}+\lambda_2(\mathbf{V}.\boldsymbol{\nabla}(\boldsymbol{\nabla}.\boldsymbol{q})+\boldsymbol{\nabla}\mathbf{V}:\boldsymbol{\nabla}\boldsymbol{q}-\boldsymbol{\nabla}\boldsymbol{q}:\boldsymbol{\nabla}\boldsymbol{V}-\boldsymbol{q}.\boldsymbol{\nabla}(\boldsymbol{\nabla}.\boldsymbol{V})+\boldsymbol{q}.\boldsymbol{\nabla}(\boldsymbol{\nabla}.\boldsymbol{V})\\ +(\boldsymbol{\nabla}.\boldsymbol{V})(\boldsymbol{\nabla}.\boldsymbol{q}))=-k\nabla^2\mathrm{T}+(h_s\boldsymbol{\nabla}.j_s+j_s.\boldsymbol{\nabla}h_s)\end{aligned} \tag{1.39}$$

$$\boldsymbol{\nabla}.\boldsymbol{q}+\lambda_2(\mathbf{V}.\boldsymbol{\nabla}(\boldsymbol{\nabla}.\boldsymbol{q})+(\boldsymbol{\nabla}.\boldsymbol{V})(\boldsymbol{\nabla}.\boldsymbol{q}))=-k\nabla^2\mathrm{T}+h_s\boldsymbol{\nabla}.j_s+j_s.\boldsymbol{\nabla}h_s \tag{1.40}$$

$$\boldsymbol{\nabla}.\boldsymbol{q}+\lambda_2(\boldsymbol{\nabla}.\{(\boldsymbol{\nabla}.\boldsymbol{q})\boldsymbol{V}\})=-k\nabla^2\mathrm{T}+h_s\boldsymbol{\nabla}.j_s+j_s.\boldsymbol{\nabla}h_s \tag{1.41}$$

From equation (1.33) replace the value of $\boldsymbol{\nabla}.\boldsymbol{q}$ in above equation,

$$\begin{aligned}-\rho C_p\left(\frac{\partial T}{\partial t}+\boldsymbol{V}.\boldsymbol{\nabla}T\right)+h_s\boldsymbol{\nabla}.j_s+\lambda_2\left(\boldsymbol{\nabla}.\left\{\left(-\rho C_p\left(\frac{\partial T}{\partial t}+\boldsymbol{V}.\boldsymbol{\nabla}T\right)+h_s\boldsymbol{\nabla}.j_s\right)\boldsymbol{V}\right\}\right)\\ =-k\nabla^2\mathrm{T}+h_s\nabla.j_s+j_s.\nabla h_s\end{aligned} \tag{1.42}$$

$$\begin{aligned}\rho C_p\left(\frac{\partial T}{\partial t}+\boldsymbol{V}.\boldsymbol{\nabla}T\right)+\lambda_2\left(\boldsymbol{\nabla}.\left\{\left(-\rho C_p\left(\frac{\partial T}{\partial t}+\boldsymbol{V}.\boldsymbol{\nabla}T\right)+h_s\boldsymbol{\nabla}.j_s\right)\boldsymbol{V}\right\}\right)\\ =-k\nabla^2\mathrm{T}+j_s.\boldsymbol{\nabla}h_s\end{aligned} \tag{1.43}$$

For steady flow$\Longrightarrow\frac{\partial \boldsymbol{q}}{\partial t}=0$,

$$\rho C_p(\boldsymbol{V}.\boldsymbol{\nabla}T)+\lambda_2\left(\boldsymbol{\nabla}.\left\{\left(-\rho C_p(\boldsymbol{V}.\boldsymbol{\nabla}T)+h_s\boldsymbol{\nabla}.j_s\right)\boldsymbol{V}\right\}\right)=-k\nabla^2\mathrm{T}+j_s.\boldsymbol{\nabla}h_s \tag{1.44}$$

Now solve this part first,

$$\begin{aligned}\boldsymbol{\nabla}.\{(-\rho C_p(\boldsymbol{V}.\boldsymbol{\nabla}T)+h_s\boldsymbol{\nabla}.j_s)\boldsymbol{V}\}\\ =(-\rho C_p(\boldsymbol{V}.\boldsymbol{\nabla}T)+h_s\boldsymbol{\nabla}.j_s)\boldsymbol{\nabla}.\mathbf{V}+\mathbf{V}.\boldsymbol{\nabla}(-\rho C_p(\boldsymbol{V}.\boldsymbol{\nabla}T)+h_s\boldsymbol{\nabla}.j_s)\end{aligned} \tag{1.45}$$

As $\boldsymbol{\nabla}.\mathbf{V}=0$,

$$\begin{aligned}\boldsymbol{\nabla}.\{(-\rho C_p(\boldsymbol{V}.\boldsymbol{\nabla}T)+h_s\boldsymbol{\nabla}.j_s)\boldsymbol{V}\}&=\mathbf{V}.\boldsymbol{\nabla}(-\rho C_p(\boldsymbol{V}.\boldsymbol{\nabla}T)+h_s\boldsymbol{\nabla}.j_s)\\ &=\mathbf{V}.\left(\boldsymbol{\nabla}\left(-\rho C_p(\boldsymbol{V}.\boldsymbol{\nabla}T)\right)+\boldsymbol{\nabla}(h_s\boldsymbol{\nabla}.j_s)\right)\end{aligned} \tag{1.46}$$

We have $h_s=C_pT$ and $j_s=-\rho_s D_B\boldsymbol{\nabla}C-\rho_s\frac{D_T}{T_\infty}\boldsymbol{\nabla}T$ so, $h_s\boldsymbol{\nabla}.j_s=C_pT\left(-\rho_s D_B\nabla^2C-\rho_s\frac{D_T}{T_\infty}\nabla^2T\right)$

and $\boldsymbol{\nabla}(h_s\boldsymbol{\nabla}.j_s)=\left(-\rho_s D_B\nabla^2C-\rho_s\frac{D_T}{T_\infty}\nabla^2T\right)\boldsymbol{\nabla}C_pT+C_pT\boldsymbol{\nabla}\left(-\rho_s D_B\nabla^2C-\rho_s\frac{D_T}{T_\infty}\nabla^2T\right)$

Replace the value of $\boldsymbol{\nabla}(h_s\boldsymbol{\nabla}.j_s)$ in equation (1.46)

$$\begin{aligned}\boldsymbol{\nabla}.\{(-\rho C_p(\boldsymbol{V}.\boldsymbol{\nabla}T)+h_s\boldsymbol{\nabla}.j_s)\boldsymbol{V}\}\\ =\mathbf{V}.\left(\boldsymbol{\nabla}\left(-\rho C_p(\boldsymbol{V}.\boldsymbol{\nabla}T)\right)+\left(-\rho_s D_B\nabla^2C-\rho_s\frac{D_T}{T_\infty}\nabla^2T\right)C_p\boldsymbol{\nabla}T\right.\\ \left.+C_pT\left(-\rho_s D_B\boldsymbol{\nabla}^3C-\rho_s\frac{D_T}{T_\infty}\boldsymbol{\nabla}^3T\right)\right)\end{aligned} \tag{1.47}$$

$$\begin{aligned}\boldsymbol{\nabla}.\{(-\rho C_p(\boldsymbol{V}.\boldsymbol{\nabla}T)+h_s\boldsymbol{\nabla}.j_s)\boldsymbol{V}\}\\ =\mathbf{V}.\left(-(\rho C_p)_f\boldsymbol{\nabla}(\boldsymbol{V}.\boldsymbol{\nabla}T)+\left(-D_B\nabla^2C-\frac{D_T}{T_\infty}\nabla^2T\right)(\rho C_p)_s\boldsymbol{\nabla}T\right.\\ \left.+(\rho C_p)_s\left(-D_BT\boldsymbol{\nabla}^3C-\frac{D_T}{T_\infty}T\boldsymbol{\nabla}^3T\right)\right)\end{aligned} \tag{1.48}$$

$$\boldsymbol{\nabla}.\{(-\rho C_p(\boldsymbol{V}.\boldsymbol{\nabla}T)+h_s\boldsymbol{\nabla}.j_s)\boldsymbol{V}\}$$
$$= -(\rho C_p)_f \mathbf{V}.\{\boldsymbol{\nabla}(\boldsymbol{V}.\boldsymbol{\nabla}T)\}$$
$$+ (\rho C_p)_s \left\{\mathbf{V}.\left(-D_B\nabla^2 C - \frac{D_T}{T_\infty}\nabla^2 T\right)\boldsymbol{\nabla}T\right. \quad (1.49)$$
$$\left. + \mathbf{V}.\left(-D_B T\boldsymbol{\nabla}^3 C - \frac{D_T}{T_\infty}T\boldsymbol{\nabla}^3 T\right)\right\}$$

Replace this value in equation (1.44)

$$(\rho C_p)_f(\boldsymbol{V}.\boldsymbol{\nabla}T) + \lambda_2\left(-(\rho C_p)_f \mathbf{V}.\{\boldsymbol{\nabla}(\boldsymbol{V}.\boldsymbol{\nabla}T)\}\right.$$
$$+ (\rho C_p)_s\left\{\mathbf{V}.\left(-D_B\nabla^2 C - \frac{D_T}{T_\infty}\nabla^2 T\right)\boldsymbol{\nabla}T\right. \quad (1.50)$$
$$\left.\left. + \mathbf{V}.\left(-D_B T\boldsymbol{\nabla}^3 C - \frac{D_T}{T_\infty}T\boldsymbol{\nabla}^3 T\right)\right\}\right) = -k\nabla^2\mathrm{T} + j_s.\boldsymbol{\nabla}h_s$$

Replace the value of $j_s.\boldsymbol{\nabla}h_s = \left(-\rho_s D_B\boldsymbol{\nabla}C - \rho_s\frac{D_T}{T_\infty}\boldsymbol{\nabla}T\right).C_p\boldsymbol{\nabla}T$ in above equation

$$(\rho C_p)_f(\boldsymbol{V}.\boldsymbol{\nabla}T) + \lambda_2\left(-(\rho C_p)_f \mathbf{V}.\{\boldsymbol{\nabla}(\boldsymbol{V}.\boldsymbol{\nabla}T)\} + (\rho C_p)_s\left\{\mathbf{V}.\left(-D_B\nabla^2 C -\right.\right.\right.$$
$$\left.\left.\left.\frac{D_T}{T_\infty}\nabla^2 T\right)\boldsymbol{\nabla}T + \mathbf{V}.\left(-D_B T\boldsymbol{\nabla}^3 C - \frac{D_T}{T_\infty}T\boldsymbol{\nabla}^3 T\right)\right\}\right) = -k\nabla^2\mathrm{T} + \left(-\rho_s D_B\boldsymbol{\nabla}C - \quad (1.51)$$
$$\left.\rho_s\frac{D_T}{T_\infty}\boldsymbol{\nabla}T\right).C_p\boldsymbol{\nabla}T$$

$$(\rho C_p)_f(\boldsymbol{V}.\boldsymbol{\nabla}T) + \lambda_2\left(-(\rho C_p)_f \mathbf{V}.\{\boldsymbol{\nabla}(\boldsymbol{V}.\boldsymbol{\nabla}T)\} + (\rho C_p)_s\left\{\mathbf{V}.\left(-D_B\nabla^2 C -\right.\right.\right.$$
$$\left.\left.\left.\frac{D_T}{T_\infty}\nabla^2 T\right)\boldsymbol{\nabla}T + \mathbf{V}.\left(-D_B T\boldsymbol{\nabla}^3 C - \frac{D_T}{T_\infty}T\boldsymbol{\nabla}^3 T\right)\right\}\right) = \quad (1.52)$$
$$-k\nabla^2\mathrm{T} + (\rho C_p)_s\left(-D_B\boldsymbol{\nabla}C.\boldsymbol{\nabla}T - \frac{D_T}{T_\infty}\boldsymbol{\nabla}T.\boldsymbol{\nabla}T\right)$$

It is the vector form of Cattaneo Christov heat flux model for nanofluid. In order to get its partial differential equation put the values of $\boldsymbol{\nabla}$ opretaor.

$$
\begin{aligned}
u\frac{\partial T}{\partial x}+v\frac{\partial T}{\partial y}+\lambda_2\Bigg[&u^2\frac{\partial^2 T}{\partial x^2}+v^2\frac{\partial^2 T}{\partial y^2}+2uv\frac{\partial^2 T}{\partial x\partial y}+\left(u\frac{\partial u}{\partial x}+v\frac{\partial u}{\partial y}\right)\frac{\partial T}{\partial x}\\
&+\left(u\frac{\partial v}{\partial x}+v\frac{\partial v}{\partial y}\right)\frac{\partial T}{\partial y}\\
&+\frac{(\rho c_p)_s}{(\rho c_p)_f}\Bigg(D_B u\left(\frac{\partial^2 C}{\partial x^2}+\frac{\partial^2 C}{\partial y^2}\right)\frac{\partial T}{\partial x}+D_B v\left(\frac{\partial^2 C}{\partial x^2}+\frac{\partial^2 C}{\partial y^2}\right)\frac{\partial T}{\partial y}\\
&+\frac{D_T}{T_\infty}u\left(\frac{\partial^2 T}{\partial x^2}+\frac{\partial^2 T}{\partial y^2}\right)\frac{\partial T}{\partial x}+\frac{D_T}{T_\infty}v\left(\frac{\partial^2 T}{\partial x^2}+\frac{\partial^2 T}{\partial y^2}\right)\frac{\partial T}{\partial y}+D_B T u\frac{\partial^3 C}{\partial x^3}\\
&+D_B T u\frac{\partial^3 C}{\partial x\partial y^2}+D_B T v\frac{\partial^3 C}{\partial y\partial x^2}+D_B T v\frac{\partial^3 C}{\partial y^3}+\frac{D_T}{T_\infty}T u\frac{\partial^3 T}{\partial x^3}\\
&+\frac{D_T}{T_\infty}T u\frac{\partial^3 T}{\partial x\partial y^2}+\frac{D_T}{T_\infty}T v\frac{\partial^3 T}{\partial y\partial x^2}+\frac{D_T}{T_\infty}T v\frac{\partial^3 T}{\partial y^3}\Bigg)\Bigg]\\
&=\frac{k}{(\rho c)_f}\left(\frac{\partial^2 T}{\partial x^2}+\frac{\partial^2 T}{\partial y^2}\right)\\
&+\frac{(\rho c)_s}{(\rho c)_f}\left[D_B\left(\frac{\partial T}{\partial x}\frac{\partial C}{\partial x}+\frac{\partial T}{\partial y}\frac{\partial C}{\partial y}\right)+\frac{D_T}{T_\infty}\left(\frac{\partial T}{\partial x}\right)^2+\frac{D_T}{T_\infty}\left(\frac{\partial T}{\partial y}\right)^2\right]
\end{aligned}
\tag{1.53}
$$

Use the boundary layer assumptions, the order of magnitude. The above equation (1.53) becomes

$$
\begin{aligned}
u\frac{\partial T}{\partial x}+v\frac{\partial T}{\partial y}+\lambda_2\Bigg[&u^2\frac{\partial^2 T}{\partial x^2}+v^2\frac{\partial^2 T}{\partial y^2}+2uv\frac{\partial^2 T}{\partial x\partial y}+\left(u\frac{\partial u}{\partial x}+v\frac{\partial u}{\partial y}\right)\frac{\partial T}{\partial x}\\
&+\left(u\frac{\partial v}{\partial x}+v\frac{\partial v}{\partial y}\right)\frac{\partial T}{\partial y}\\
&+\frac{(\rho c_p)_s}{(\rho c_p)_f}\Bigg(D_B u\frac{\partial^2 C}{\partial y^2}\frac{\partial T}{\partial x}+D_B v\frac{\partial^2 C}{\partial y^2}\frac{\partial T}{\partial y}+\frac{D_T}{T_\infty}u\frac{\partial^2 T}{\partial y^2}\frac{\partial T}{\partial x}\\
&+\frac{D_T}{T_\infty}v\frac{\partial^2 T}{\partial y^2}\frac{\partial T}{\partial y}+D_B T u\frac{\partial^3 C}{\partial x\partial y^2}+D_B T v\frac{\partial^3 C}{\partial y^3}+\frac{D_T}{T_\infty}T u\frac{\partial^3 T}{\partial x\partial y^2}\\
&+\frac{D_T}{T_\infty}T v\frac{\partial^3 T}{\partial y^3}\Bigg)\Bigg]\\
&=\frac{k}{(\rho c)_f}\left(\frac{\partial^2 T}{\partial y^2}\right)+\frac{(\rho c)_s}{(\rho c)_f}\left[D_B\left(\frac{\partial T}{\partial y}\frac{\partial C}{\partial y}\right)+\frac{D_T}{T_\infty}\left(\frac{\partial T}{\partial y}\right)^2\right]
\end{aligned}
\tag{1.54}
$$

So above equation is the partial differential equation of Cattaneo christov heat flux model with nanofluids.

- **Equation of Transportation of nanoparticles**

Now the equation for nanoparticle concentration without any chemical reaction can be written as

$$\frac{\partial C}{\partial t} + \boldsymbol{V}.\boldsymbol{\nabla} C = -\frac{1}{\rho_s}\boldsymbol{\nabla}.j_s \tag{1.55}$$

In which C is the nanoparticle volume fraction and j_s is defined as $j_s = j_{s,B} + j_{s,T}$. Replace the value of j_s in above equation,

$$\frac{\partial C}{\partial t} + \boldsymbol{V}.\boldsymbol{\nabla} C = -\frac{1}{\rho_s}\boldsymbol{\nabla}.\left(D_B \boldsymbol{\nabla} C + D_T \frac{\boldsymbol{\nabla} T}{T_\infty}\right) \tag{1.56}$$

$$\frac{\partial C}{\partial t} + \boldsymbol{V}.\boldsymbol{\nabla} C = \left(D_B \nabla^2 C + D_T \frac{\nabla^2 T}{T_\infty}\right) \tag{1.57}$$

$$\frac{\partial C}{\partial t} + u\frac{\partial C}{\partial x} + v\frac{\partial C}{\partial y} = D_B\left(\frac{\partial^2 C}{\partial x^2} + \frac{\partial^2 C}{\partial y^2}\right) + \frac{D_T}{T_\infty}\left(\frac{\partial^2 T}{\partial x^2} + \frac{\partial^2 T}{\partial y^2}\right) \tag{1.58}$$

We are considering the steady state flow and after using boundary layer assumptions, the order of magnitude. The above equation becomes

$$u\frac{\partial C}{\partial x} + v\frac{\partial C}{\partial y} = D_B\left(\frac{\partial^2 C}{\partial y^2}\right) + \frac{D_T}{T_\infty}\left(\frac{\partial^2 T}{\partial y^2}\right) \tag{1.59}$$

1.5 Solution Methodology

The governing equations are partial differential equation and in order to solve these equations first of all we used similarity parameters. With the help of these parameters we will be able to convert our partial differential equation into ordinary differential equation, also these parameters non-dimensionalized our equations. After that we will take help with a renounced numerical method namely Keller-box method. This method works with the collaboration of newton's linearization technique which is described by Cebeci and Bradshanin 1948, the basic idea of Keller-box method is to write the governing equation in form of first order system. For this

purpose insert few dependent variables to decrease the order of ordinary differential equations. After that use the centered-difference scheme for the derivatives and average to get the finite difference equation [37] then apply the newton's method. The resulting equations are written in matrix vector form and these equations are solved by block tridiagonal elimination method.

Chapter 2
Simulations by homogeneous model

2.1 Introduction

In this chapter we discussed about the flow and heat transfer of non-Newtonian nanofluids (upper convective Maxwell fluid) over a stretching sheet with convective boundary conditions. We are considering Ethanol as a non-Newtonian fluid as its Prandtl number is 18.05. To fulfill this purpose we utilize homogeneous with using five different types of nanoparticles namely Copper Oxide (CuO), Copper (Cu), Sliver (Ag), Titanium Oxide (TiO_2), Alumina ($AI_2\ O_3$). For heat transport Catteno-Christov heat flux model is considered by us. The performance of different parameters such as stretching parameter, thermal relaxation parameter, suction parameter and Biot number are examined and exhibits their action by plotting graphs.

2.2 Problem Statement

Investigate the flow and heat transfer behaviour of Maxwell nanofluid incorporate with Cattaneo Christov heat flux model.

2.3 Mathematical Modeling

Let us consider 2-dimension incompressible, steady flow of non-Newtonian nanofluid over a stretching sheet. Fluid is moving due to the stretching and suction of surface. Convective heat transfer is also considered due to the presence of hot fluid which is below the surface.

The derivation of governing equations of mass, momentum and energy by using the homogeneous is discussed in chapter 1 (equation 1.9, 1.22 and 1.27) these equations are given below:

$$\frac{\partial u}{\partial x}+\frac{\partial v}{\partial y}=0 \tag{1.9}$$

$$u\frac{\partial u}{\partial x}+v\frac{\partial u}{\partial y}+\lambda_1\left(u^2\frac{\partial^2 u}{\partial x^2}+2uv\frac{\partial^2 u}{\partial x\partial y}+v^2\frac{\partial^2 u}{\partial y^2}\right)=\frac{\mu_{nf}}{\rho_{nf}}\left(\frac{\partial^2 u}{\partial y^2}\right) \tag{1.22}$$

$$u\frac{\partial T}{\partial x}+v\frac{\partial T}{\partial y}+\lambda_2\left[u^2\frac{\partial^2 T}{\partial x^2}+v^2\frac{\partial^2 T}{\partial y^2}+2uv\frac{\partial^2 T}{\partial x\partial y}+\left(u\frac{\partial u}{\partial x}+v\frac{\partial u}{\partial y}\right)\frac{\partial T}{\partial x}+\left(u\frac{\partial v}{\partial x}+v\frac{\partial v}{\partial y}\right)\frac{\partial T}{\partial y}\right]=\alpha_{nf}\left(\frac{\partial^2 T}{\partial y^2}\right) \tag{1.27}$$

Where ρ_{nf} the density of nanofluid is, μ_{nf} is the dynamic viscosity of nanofluid, α_{nf} is the thermal diffusivity of nanofluid.

Boundary conditions for our problem are given below

$$u=ax,\quad v=-V_s,\quad -k_{nf}\frac{\partial T}{\partial y}=h_f\left(T_f-T\right),\quad at\ \ y=0$$
$$u=0,\quad T=T_\infty,\quad at\ \ y\to\infty \tag{2.1}$$

Where u, v represents the velocity components, V_s depicts the vertical velocity on surface. $V_s>0$ Shows the suction velocity, $V_s<0$ shows the injection velocity. T denotes the temperature, T_f is fluid temperature T_∞ shows the ambient temperature, h_f shows the convective heat temperature. k_{nf} is thermal conductivity which is defined in equation (1.28).

For these equations we are going to use the following similarities transformations.

$$\eta=y\sqrt{\frac{a}{\nu}},\qquad \psi=x\sqrt{a\nu}f(\eta),$$
$$\theta(\eta)=\frac{T-T_\infty}{T_w-T_\infty} \tag{2.2}$$

By using these similarities transformation, the required PDE's are transformed into following ordinary differential equations and also boundary conditions are transformed.

$$\left(\alpha_1 f^2 - \frac{1}{(1-\varphi)^{2.5}\left(1-\varphi+\varphi\frac{\rho_s}{\rho_f}\right)}\right) f''' - (1+2\alpha_1 f')ff'' + f'^2 = 0 \qquad (2.3)$$

$$\left(\frac{k_{nf} * \rho_f}{Pr\left(1-\varphi+\varphi\frac{\rho c_{p_s}}{\rho c_{p_f}}\right)} - \alpha_2 f^2\right)\theta'' + (1-\alpha_2 f')f\theta' = 0 \qquad (2.4)$$

$$f'(0) = 1, \quad f(0) = S, \quad \theta'(0) = \gamma(\theta(0)-1) \quad at \ \eta = 0$$
$$f'(\infty) = 0, \quad \theta(\infty) = 0 \qquad at \ \eta \to \infty \qquad (2.5)$$

Where $\alpha_1 = a\lambda_1$ is the relaxation parameter, $\alpha_2 = a\lambda_2$ is thermal relaxation parameter, $S = \frac{V_s}{\sqrt{a\nu}}$ is suction parameter, $Pr = \frac{(\mu c_p)_f}{k_f}$ is a Prandtl number.

Local Nusselt number and skin friction coefficient are defined as respectively $Nu_x = \frac{xq_x}{k_f(T_f - T_\infty)}$, $C_f = \frac{\tau_x}{\rho U^2}$. Where $q_x = \left(-k_{nf}\frac{\partial T}{\partial y}\Big|_{y=0}\right)$ and $\tau_x = \left(-\mu_{nf}\frac{\partial u}{\partial y}\Big|_{y=0}\right)$.

After using the non-dimensional quantities in local Nusselt number and skin friction coefficient, they transformed as:

$$Nu_x = -\theta'(0)\frac{k_{nf}}{k_f} \qquad (2.6)$$

$$C_f = \frac{1}{(1-\varphi)^{2.5}} f''(0) \qquad (2.7)$$

2.4 Numerical Solution

The system of above non-dimensionalized equations (2.3) and (2.4), of momentum and energy equations with their corresponding boundary conditions (2.5) are solved by using the Keller-box method. As our system is in form of third ordered equation so first we reduced our system of equations (2.3) and (2.4) into first order equation by inserting these new variables:

$$f' = u,\ \ u' = v,\ \ u'' = v'$$
$$\theta' = y,\ \ \theta'' = y' \tag{2.8}$$

These variables transformed our system as:

$$(\alpha_1 f^2 - cf)v' - (1 + 2\alpha_1 u)fv + u^2 = 0 \tag{2.9}$$

$$(ct - \alpha_2 f^2)y' + (1 - \alpha_2 u)fy = 0 \tag{2.10}$$

Where $cf = \frac{1}{(1-\varphi)^{2.5}\left(1-\varphi+\varphi\frac{\rho_S}{\rho_f}\right)}$ and $ct = \frac{k_{nf}*\rho_f}{Pr\left(1-\varphi+\varphi\frac{\rho c p_S}{\rho c p_f}\right)}$

Now in ordered to get the finite difference equation we use centered difference derivatives and averages, after that follow the Newton's method to linearize the non-linear system of our equations. Then these linearized difference equation write as the system of matrix vector form which is known as tridiagonal matrix form and these matrices solved by using Block-Elimination method. For this purpose use the MATLAB code with tolerance $10^{-6.}$

2.5 Numerical Results and Discussion

Before keeping an eye on the results of physical effects we are going to validate our results with the previous knowledge. For the purpose of affirmation taking the value of skin friction coefficient with Abel et al. [38], Megahed et al. [39], Sadeghy et al. [40], Mukhopadhyay et al. [23], Shahid et al. [23]. These values are calculated for $\alpha_1 = 0 = M$, which negates the presences of relaxation parameter and magnetic field. Table 2.1 performs the association of the present results with the previous knowledge and the results of the given table show the reasonable settlement. Table 2.2 has thermo physical properties of non-Newtonian fluid (Ethanol) with few nanoparticles.

Table 2.1 comparison of skin friction between the previous knowledge with the present results for $\alpha_1 = 0 = M$

	Abel et al. [38]	**Megahedet al.** [39]	**Sadeghy et al.** [40]	**Mukhopadhyay et al.** [23]	**Shahid et al.** [23]	**Present results**
C_{fx}	-0.999962	-0.999978	-1.000000	-0.999996	-1.000000	-1.000000

Table 2.2 Thermo physical properties of non-Newtonian fluid and few nanoparticles

	$c_p(Jkg^{-1}K^{-1})$	$\rho(kgm^{-3})$	$k(Wm^{-1}K^{-1})$
Ethanol	2840	789	0.169
Silver (Ag)	235	10500	429
Titanium Oxide(TiO_2)	686.2	4250	8.9538
Copper oxide (CuO)	531.8	6320	76.5
Copper (Cu)	385	8933	401
Alumina (Al_2O_3)	765	3970	40

Now the focus on the investigation of the physical effects for the multiple parameters such as $\alpha_1$relaxation parameter, α_2 thermal relaxation parameter, S Suction parameter, Pr Prandtl number, Bi Biot number and for the different values of concentration φ. Figure 2.1 shows the effect of different nanofluids on $f'(\eta)$. The diagram leads us to make the conclusion that velocity boundary layer profile of Alumina Oxide is the largest among of all nanoparticles it is also noted that its density is the lowest among all, followed by Titanium Oxide. Nanoparticles of Titanium

Oxide are denser than Alumina, Copper Oxide, Copper and Silver respectively, on the other hand there boundary layer thickness are smaller. The figure shows that the thickness of the velocity boundary layer profile depends on density. Figure 2.2, 2.3 shows the behavior of velocity boundary layer profile for Alumina Oxide and Silver with different values of phi. Figure 2.2 portrait that increment in concentration does not leaves a major impact on profile, on the other hand in figure 2.3 increment in concentration does leaves a major impact on profile for silver based nanofluid. As we know that the density of Alumina Oxide is less than the others. Therefore, velocity boundary layer profile with the augmentation of concentration is clearly affected by density of nanoparticles and showed that concentration influence is significant for denser nanoparticles. Increasing nanoparticle concentration reduces velocity boundary layer and this behavior is significant in denser nanoparticle. Figure 2.4 represents the effects of thermal boundary layer with the variation of concentration and thermal relaxation parameter. With the advancement of thermal relaxation parameter thermal boundary layer decreases and opposite behavior depicted by increasing concentration. Figure 2.5 shows the positive impact on the thermal boundary layer with the increment of Biot number and this actions remains the consistence with the rest of nanofluids. Increasing suction decrease thermal boundary layer which is clearly seen by figure 2.6 and this effect is not only valid for Copper Oxide nanofluid but also for all other nanoparticles. Figure 2.7 and 2.8 shows the behavior of thermal relaxation parameter and concentration of nanoparticles for different values of Biot number. As the behavior of these parameters is almost same for all nanoparticles so here it is only given with the copper. It is clearly depicted in figure, that the increasing values of concentration, thermal relaxation parameter and Biot number, profile of Nusselt number is showing increasing behavior for these parameters. Figure 2.8 shows the percentage difference in Fig. 2.7 we can observe same slope for all profile however Fig. 2.8 display that increasing relaxation parameter and Biot number reduce profile slope/rate of change. Variation of relaxation parameter does not leaves a significant impact on rate of change of surface temperature whereas suction parameter shows the significant impact as depict in Fig. 2.9, the effect of relaxation parameter remains same for all nanofluids considered. Figure 2.10 depicts the effect of relaxation parameter, suction as a function of concentration in terms of percentage difference to observe rate of change, with increasing value of relaxation parameter slop of local Nusselt number decreases and it also decreases with suction. Figure 2.11 portrait effects of relaxation parameter and suction both

influence the skin friction coefficient. As they arise so do the coefficient. Table 2.3 shows the numerical results of Nusselt number with the various values of different parameters for five different nanofluids.

2.6 Conclusion

Effects of Upper-Convective Maxwell nanofluid with Cattaneo Christov heat flux model is examined in this chapter. Numerical computations are performed by Keller-box method. The major points of this work are summarized below:

1. Relaxation parameter is an increasing function of skin friction coefficient.
2. Skin friction coefficient and Nusselt number are increasing function of concentration.
3. Increase in thermal relaxation parameter increases Nusselt number
4. Increase in Biot number increases thermal penetration depth and Nusselt number.
5. Increase in Suction parameter increases skin friction coefficient and Nusselt number.
6. The slope of Nusselt number reduces with relaxation parameter (α_1), thermal relaxation parameter (α_2), Biot number (Bi) and suction (S).

Table 2.3 Results of Nusselt number with variation of different parameters for five different nanofluids

φ	α_1	α_2	S	Bi	Ag-Ethanol	TiO_2-Ethanol	CuO - Ethanol	Cu - Ethanol	Al_2O_3-Ethanol
0.05	0.5	0.05	0.4	10	5.4631	5.4877	5.5289	5.5295	5.5118
0.1					5.8223	5.8827	5.9688	5.9691	5.9325
0.2					6.5369	6.6981	6.8874	6.8853	6.8059
0.1	0.1				5.8586	5.9038	5.9942	6.0002	5.9534
	0.5				5.8223	5.8827	5.9688	5.9691	5.9325
	0.5	0.01			5.4827	5.5359	5.6149	5.6137	5.5841
		0.05			5.8223	5.8827	5.9688	5.9691	5.9325
		0.05	0		3.5452	3.6051	3.6462	3.6340	3.6383
			0.4		5.8223	5.8827	5.9688	5.9691	5.9325
			0.4	5	4.0522	4.0628	4.1207	4.1228	4.1013
				10	5.8223	5.8827	5.9688	5.9691	5.9325

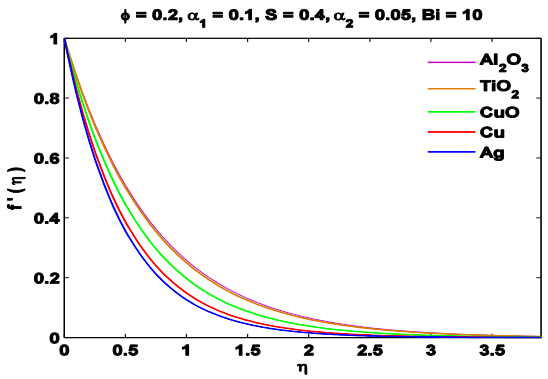

Figure 2.1 Effect of different nanofluids on $f'(\eta)$

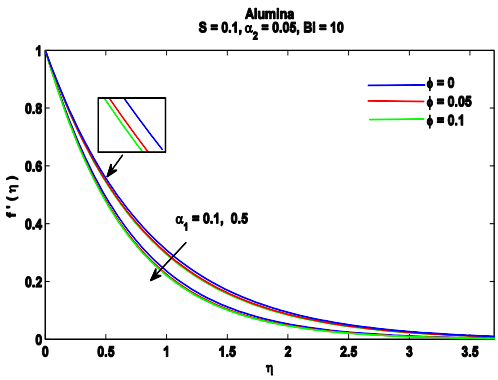

Figure 2.2 Effect of Alumina AI_2O_3 with α_1 on $f'(\eta)$ for different values of φ

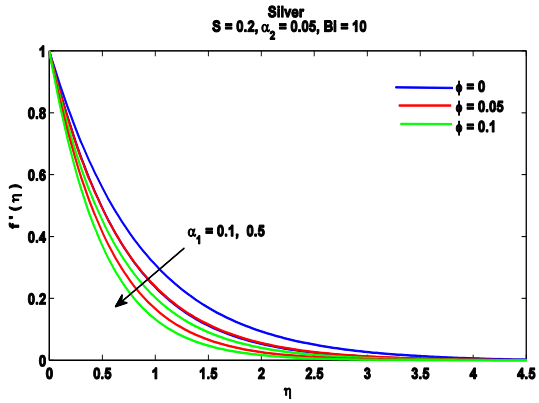

Figure 2.3 Effect of Silver Ag with α_1 on $f'(\eta)$ for different values of φ

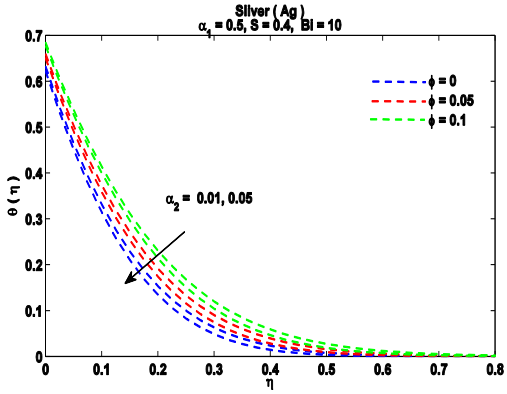

Figure 2.4 Effect of Silver Ag with α_2 on $\theta(\eta)$ for different values of φ

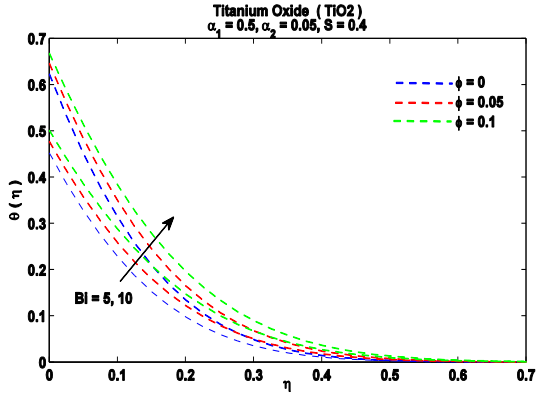

Figure 2.5 Effect of Titanium Oxide with Bi on $\theta(\eta)$ for different values of φ

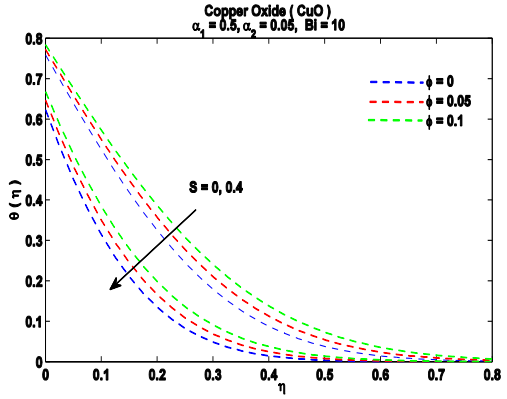

Figure 2.6 Effect of Copper Oxide (CuO) with S on $\theta(\eta)$ for different values of φ

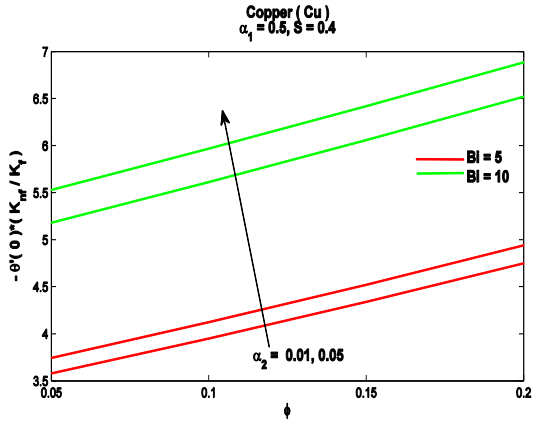

Figure 2.7 Effect of Copper (Cu) with α_2 and φ on local Nusselt number for different values of Bi

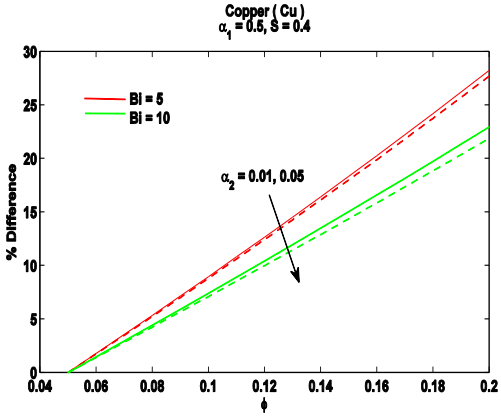

Figure 2.8% Difference of copper *(Cu)* with α_2 and φ on local Nusselt number for different values of Bi

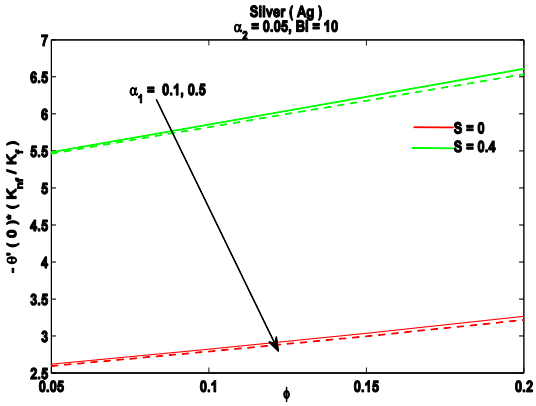

Figure 2.9 Effect of Silver (Ag) with α_1 and φ on local Nusselt number for different values of S

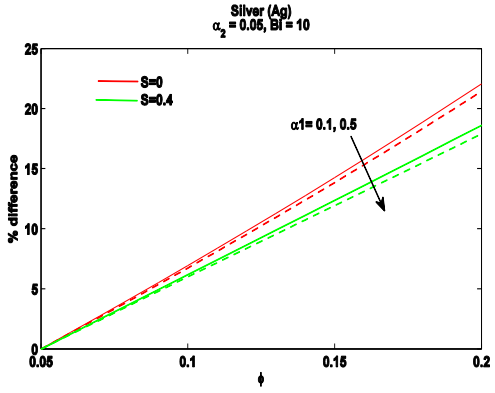

Figure 2.10 % Difference of Silver (Ag) with α_1 and φ on local Nusselt number for different values of S

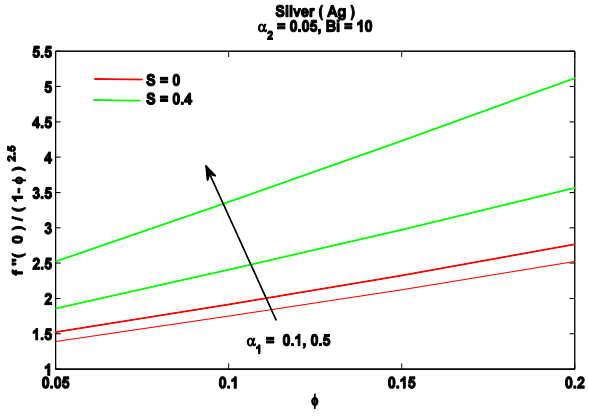

Figure 2.11 Effect of Silver ***Ag*** with $\boldsymbol{\alpha_1}$ and $\boldsymbol{\varphi}$ on skin friction coefficient for different values of S

Chapter 3
Simulations by non-homogeneous model

3.1 Introduction

This chapter deals with the same problem as in chapter 2 the difference is the nanofluid model in the previous chapter we used homogeneous (Tiwari Das) model however in this chapter we are using non-homogeneous (Buongiorno) model along with standard Cattaneo Christov heat flux model. This model shows the importance of Brownian diffusion and thermophoresis parameter. Suitable similarity transformation leads us towards the system of non-linear differential equation. This system is solved numerically by using the Keller-box method.

3.2 Problem Formulation

Let us considered the 2-dimension, steady, incompressible flow over linearly stretching sheet. The sheet is stretching in x-direction with velocity $u = ax$ where a is constant, also suction effects considered on surface $v = -V_s$. Maxwell model is considered for Maxwell fluid and for heat transfer Cattaneo-Christov model is considered. Let T shows the temperature whereas T_w be the surface temperature and T_∞ denotes the ambient temperature of fluid. Let C shows the concentration of nanoparticle whereas C_w depicts the concentration of nanoparticle on surface and C_∞ denotes the ambient concentration of nanoparticles.

After considering the non-homogeneous model for nanofluids, we can express our equations of conservation of mass, momentum and energy in form of partial differential equation as (discussed the derivation in chapter 1, equation 1.9, 1.21 1.32 and 1.59):

$$\frac{\partial u}{\partial x} + \frac{\partial v}{\partial y} = 0 \qquad (1.9)$$

$$u\frac{\partial u}{\partial x}+v\frac{\partial u}{\partial y}+\lambda_1\left(u^2\frac{\partial^2 u}{\partial x^2}+2uv\frac{\partial^2 u}{\partial x\partial y}+v^2\frac{\partial^2 u}{\partial y^2}\right)=\nu\left(\frac{\partial^2 u}{\partial y^2}\right) \tag{1.21}$$

Where u, v represents the velocity component along x, y −axis, λ_1 is the fluid relaxation time, ν is the kinematic viscosity.

$$\begin{aligned} u\frac{\partial T}{\partial x}+v\frac{\partial T}{\partial y}+\lambda_2\Bigg[&u^2\frac{\partial^2 T}{\partial x^2}+v^2\frac{\partial^2 T}{\partial y^2}+2uv\frac{\partial^2 T}{\partial x\partial y}+\left(u\frac{\partial u}{\partial x}+v\frac{\partial u}{\partial y}\right)\frac{\partial T}{\partial x}\\ &+\left(u\frac{\partial v}{\partial x}+v\frac{\partial v}{\partial y}\right)\frac{\partial T}{\partial y}\Bigg]\\ &=\frac{k}{(\rho c)_f}\left(\frac{\partial^2 T}{\partial y^2}\right)+\frac{(\rho c)_p}{(\rho c)_f}\left[D_B\left(\frac{\partial T}{\partial y}\frac{\partial C}{\partial y}\right)+\frac{D_T}{T_\infty}\left(\frac{\partial T}{\partial y}\right)^2\right] \end{aligned} \tag{1.32}$$

Where u, v are the velocity component along x, y −axis respectively, T is temperature, λ_2 is a thermal relaxation time, k is a thermal conductivity, $(\rho c)_f$ is the specific heat capacity of base fluid, $(\rho c)_s$ is the specific heat capacity of particles, D_B is Brownian diffusion coefficient, D_T is the Thermophoretic diffusion coefficient and T_∞ shows the ambient temperature.

$$u\frac{\partial C}{\partial x}+v\frac{\partial C}{\partial y}=D_B\left(\frac{\partial^2 C}{\partial y^2}\right)+\frac{D_T}{T_\infty}\left(\frac{\partial^2 T}{\partial y^2}\right) \tag{1.59}$$

Where u, v represents the velocity components, C is the nanoparticles concentration, D_B is Brownian diffusion coefficient, D_T is the Thermophoretic diffusion coefficient and T_∞ shows the ambient temperature.

Now the required boundary conditions for the considered specific problem are

$$\begin{aligned} &u=ax,\quad v=-V_s,\quad -k\frac{\partial T}{\partial y}=h_f\left(T_f-T\right),\quad \frac{\partial C}{\partial y}=0 \quad at\ y=0\\ &u=0,\qquad T=T_\infty,\qquad C=C_\infty \qquad\qquad at\ y\to\infty \end{aligned} \tag{3.1}$$

In which k is a thermal conductivity, h_f is the convective heat transfer coefficient of fluid and T_f is fluid temperature. In the above equations using the following suitable similarity transformation,

$$\eta = y\sqrt{\frac{a}{\nu}}\,, \qquad \psi = x\sqrt{a\nu}f(\eta), \tag{2.2}$$

$$\theta(\eta) = \frac{T - T_\infty}{T_w - T_\infty}, \qquad \varphi(\eta) = \frac{C - C_\infty}{C_w - C_\infty} \tag{3.2}$$

By using the given similarities transformation, Eq. (1.9) identically satisfy and the required PDE's are transformed into following ordinary differential equations and also boundary conditions are transformed .

$$(1 - \alpha_1 f^2)f''' + (1 + 2\alpha_1 f')ff'' - f'^2 = 0 \tag{3.3}$$

$$\left(\frac{1}{Pr} - \alpha_2 f^2\right)\theta'' + (1 - \alpha_2 f')f\theta' + Nb\theta'\varphi' + Nt\theta'^2 = 0 \tag{3.4}$$

$$\varphi'' + \frac{Nt}{Nb}\theta'' + Scf\varphi' = 0 \tag{3.5}$$

$$\begin{gathered} f'(0) = 1, \quad f(0) = S, \quad \theta'(0) = Bi(\theta(0) - 1), \quad \varphi'(0) = 0 \quad at\ \eta = 0 \\ f'(\infty) = 0, \quad \theta(\infty) = 0, \quad \varphi(\infty) = 0 \quad at\ \eta \to \infty \end{gathered} \tag{3.6}$$

Where α_1 is the elasticity parameter, α_2 is the thermal relaxation parameter, $Pr = \nu/\alpha$ is a Prandtl number, $Nb = D_B(\rho c)_p(C_w - C_\infty)/(\rho c)_f\nu$ is the Brownian motion parameter, $Nt = D_T(\rho c)_p(T_w - T_\infty)/(\rho c)_f T_\infty\nu$ is the Thermophoresis parameter, $Sc = \nu/D_B$ is a Schmidt number, $S = V_s/\sqrt{a\nu}$ is a suction parameter and $Bi = \frac{k}{h}\sqrt{\frac{a}{\nu}}$ is Biot number.

Local Nusselt number Nu is defined as:

$$Nu_x = \frac{xq_x}{k_f(T_f - T_\infty)} \tag{3.7}$$

Where $q_x = \left(-k_{nf}\frac{\partial T}{\partial y}\Big|_{y=0}\right)$, using this local Nusselt number becomes

$$Nu_x = -\theta'(0) \tag{3.8}$$

Skin friction coefficient C_f also defined as:

$$C_f = \frac{\tau_x}{\rho U^2} \tag{3.9}$$

Where $\tau_x = \left(-\mu_{nf} \frac{\partial u}{\partial y}\Big|_{y=0}\right)$ and using this Skin friction coefficient becomes

$$C_f = f''(0) \tag{3.10}$$

3.3 Numerical Method

The above non-dimensionalized equations (3.3), (3.4), (3.5) of mass, momentum, energy and concentration equation with their concerned boundary conditions (3.6) are solved by using the Keller-Box method. For this purpose, firstly introduce the new dependent variables.

$$\begin{gathered} f' = u,\ \ u' = v,\ \ f''' = v' \\ \theta' = y,\ \ \theta'' = y' \\ \varphi' = z,\ \ \varphi'' = z' \end{gathered} \tag{3.11}$$

These variables transformed the above system of third ordered differential equations (3.3), (3.4), (3.5) into the system first ordered differential equation and it becomes,

$$(1 - \alpha_1 f^2)v' + (1 + 2\alpha_1 u)fv - u^2 = 0 \tag{3.12}$$

$$\left(\frac{1}{Pr} - \alpha_2 f^2\right)y' + (1 - \alpha_2 u)fy + Nbyz + Nty^2 = 0 \tag{3.13}$$

$$z' + \frac{Nt}{Nb}y' + Scfz = 0 \tag{3.14}$$

In order to gets the finite difference equation, the above equations solved by using the centered difference scheme for derivatives and averages, after that using Newton's method to linearize the non-linear system of our equations. Then these linearized difference equation write as the system of matrix vector form which is known as tridiagonal matrix form and these matrices solved by using Block-Elimination method. For this purpose use the MATLAB code with tolerance 10^{-6}.

3.4 Results and Discussions

In this section we are going to analysis the physical effects for different parameter α_1 relaxation parameter, S Suction parameter, α_2 thermal relaxation parameter, Pr is Prandtl number, Sc is Schmidt number, Nt is Thermophoresis parameter, Nb is Brownian motion parameter, Bi is Biot number. Figure 3.1 shows α_1 and S effects on velocity profile. It presents the increase in suction parameter will decrease the velocity boundary layer profile in spite of that it shows increment in case of injection. For the relaxation parameter, velocity boundary layer profile decreases with the increment in parameter. In figure 3.2 with the increasing value of α_1 temperature boundary layer profile also increases despite to that on the other hand with the increasing value of suction thermal boundary layer decreases. In case of injection thermal boundary increases and shows the opposite reaction than the suction. So from the figure 3.1 and 3.2 we can make a decision that in case of suction/injection velocity and thermal boundary layer both shows the same reaction regardless of that they both depict the contrasting behavior with relaxation parameter. Figure 3.3 illustrate decline with the increasing value of α_2 which means that if thermal relaxation time increases it shows decreasing affects on temperature boundary layer, also this figure portrait with the accumulation of thermophoresis parameter thermal boundary layer also increases. On the thermal boundary layer, Schmidt number is not showing any significant effects but with the enlarging Prandtl number it is clearly notified that thermal boundary layer depreciates, we can take this decision from figure 3.4. That means kinematic viscosity left opposite effects on temperature profile. Prandtl>10 shows non-Newtonian fluid, so if kinematic viscosity increases in non-Newtonian fluid the thickness of thermal boundary layer becomes lesser. The effect of Biot number on thermal boundary layer shows in figure 3.5. Biot number is the ratio between the convective heat transfer coefficient and the thermal conductivity. The accumulation in convective heat transfer coefficient depicts the same response in the thickness of thermal boundary layer.

The figure 3.6 – 3.10 shows the behavior of concentration profile with different parameters. Figure 3.6 shows the performance of relaxation parameter along with suction parameter on concentration boundary layer thickness. It depicts that enlarging relaxation parameter also lifting concentration profile upward side, same response is noticed for injection and against of that in

case of suction concentration profile dragging downward side. The response of Brownian motion parameter and Thermophoresis parameter is published in figure 3.7. The both parameters are showing opposite response towards each other as with the expansion of Thermophoresis parameter the thickness of concentration profile rises. But on the other hand with the accumulation in Brownian motion parameter the boundary layer profile of concentration decreases. Figure 3.8 represent the performance of Prandtl number and Schmidt number on concentration boundary layer. Schmidt number is the ratio between the viscous diffusion and mass diffusion so concentration profile shrinks due to less mass diffusion but with the thermal diffusion this profile shrinks. Biot number is the ratio of heat transfer coefficient and thermal conductivity. Concentration profile not only arises but also drags towards infinity with the addition of heat transfer coefficient; figure 3.9 clearly leaves the impact of this action. Increment in thermal relaxation parameter shows the incorporate response in concentration boundary layer profile, figure 3.10. Performance of relaxation parameter and thermal relaxation parameter for different values of suction is representing by figure 3.11. Increasing value of α_1 shows decreasing behavior in spite of that thermal relaxation parameter shows its opposite behavior, it arises with boosted values. This diagram also portrait increase in reduced Nusselt number with suction. Figure 3.12 depicts almost same rate of change for these values and these parameters have linear function. Expansion of Prandtl number illustrates development with the expanded value of Schmidt number and also for suction it is shown in figure 3.13. Figure 3.14 shows their rate of change, means for the larger values of Prandtl number increase the surface temperature but there relative rate of change will reduce, also the heat transfer rate is a non-linear function of Schmidt number. Increase in thermophorises parameter reduces the heat transfer rate as shown in figure 3.15. Thermophorises parameter is a non-linear function and with its increasing value its rate of change also increases this can be seen by figure 3.16. Figure 3.17 and 3.18 characterize the behavior of relaxation parameter and thermal relaxation parameter on $-\theta'(0)$ for Biot number, both parameter portrait declines with larger values. Nusselt number rate of change decreases with the increase of thermal relaxation parameter. On the other hand behavior of Prandtl number and Schmidt number is opposite of Biot number. Nusselt number is a non-linear function of Schmidt number and rate of change increases with bigger values of the parameters shown in figure 3.19 and 3.20. Behavior of skin friction coefficient shows by figure 3.21, increasing the value of relaxation parameter shows more resistance on surface.

Table 3.1 represents the numerical results of reduces Nusselt number with variation of different parameters.

3.5 Conclusion

This chapter studies the effects of non-homogeneous model on Upper-Convective Maxwell nanofluid with Cattaneo Christov heat flux model. The results relaxation parameter, thermal relaxation parameter, suction, and Biot number are in agreement with the previous study of chapter 2. The additional effects of non-homogeneous model are summarized below:

1. Prandtl number increase reduce the thermal boundary layer and increase Nusselt number, but the slope of Nusselt number reduces with the increase in Prandtl number.
2. Skin friction coefficient is an increasing function of relaxation parameter.
3. Thermophoresis parameter reduce Nusselt number while slope of Nusselt number increases.
4. Temperature and concentration profile increase with thermophoresis parameter.
5. Brownian motion parameter reduces concentration profile.
6. Schmidt number reduces the penetration depth of temperature and concentration but remain neutral for Nusselt number.

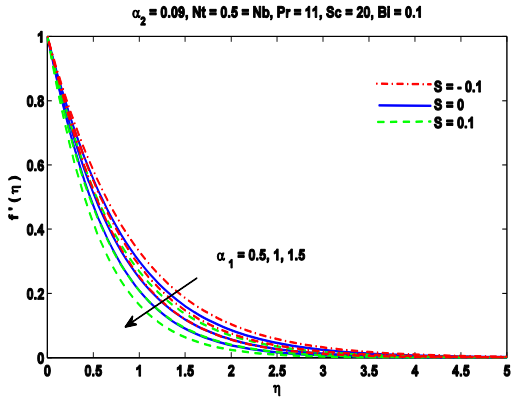

Figure 3.1 Effects of α_1 and S on f'

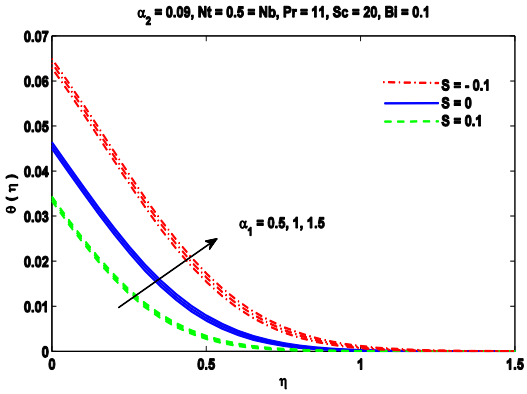

Figure 3.2 Effects of α_1 and S on θ

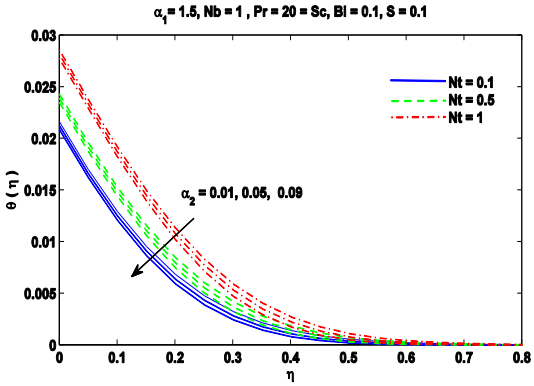

Figure 3.3 Effects of α_2 and Nt on θ

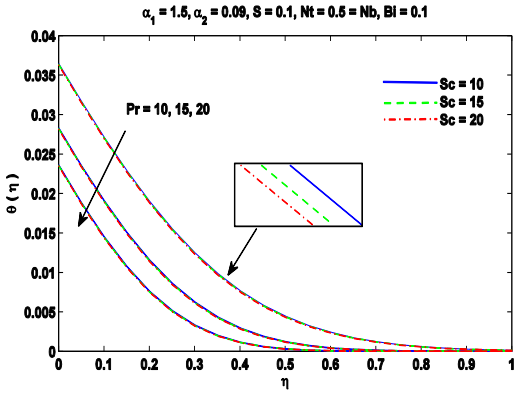

Figure 3.4 Effect of Pr and Sc on θ

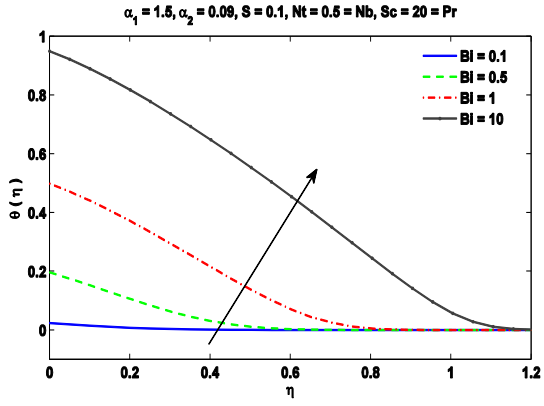

Figure 3.5 Effect of Bi on $\boldsymbol{\theta}$

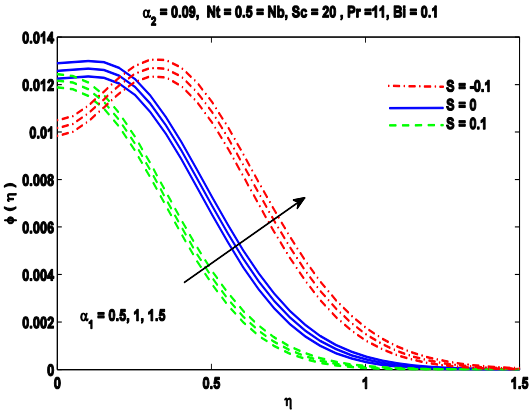

Figure 3.6 Effect α_1 and S on φ

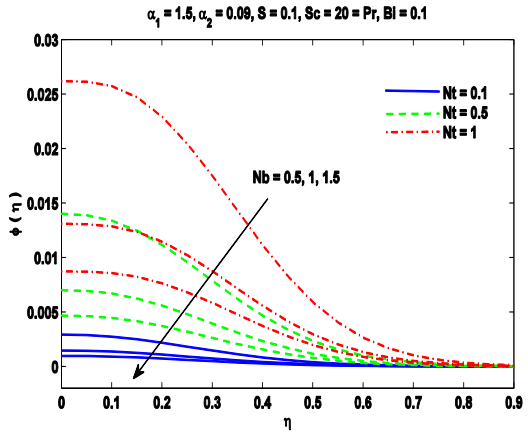

Figure 3.7 Effect of Nt, Nb on φ

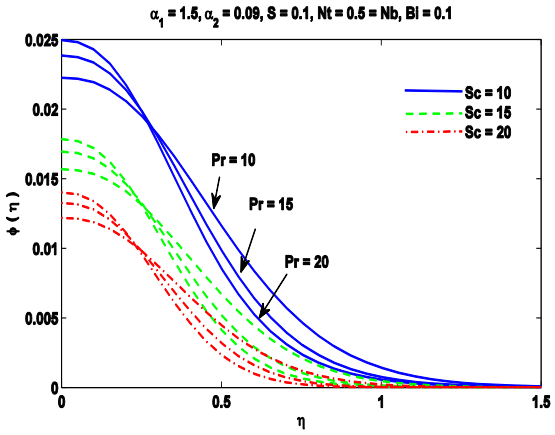

Figure 3.8 Effect of Pr and Sc on $\boldsymbol{\varphi}$

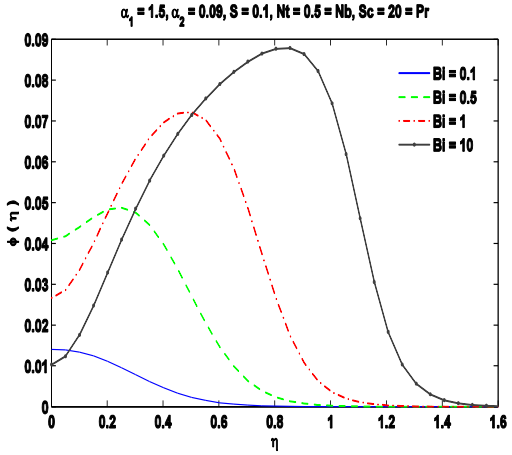

Figure 3.9 Effects of Bi on φ

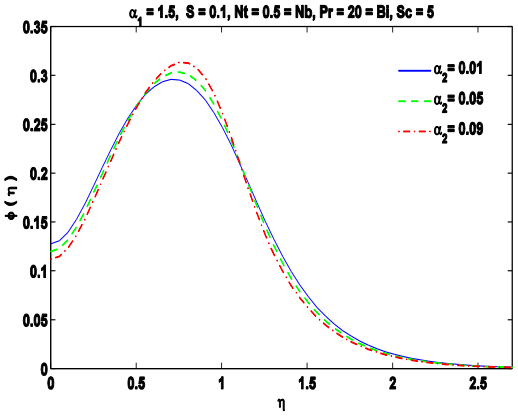

Figure 3.10 Effect of α_2 on φ

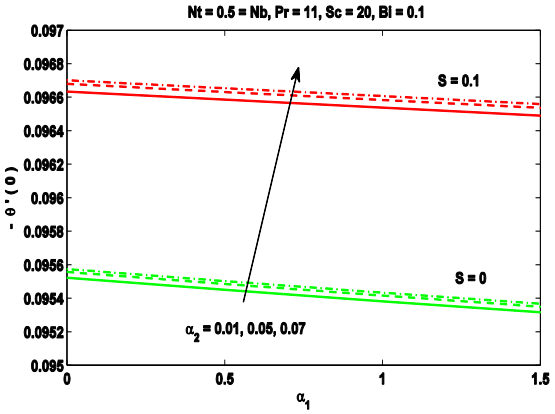

Figure 3.11 Effect of α_1, α_2 on $-\theta'(0)$ for S

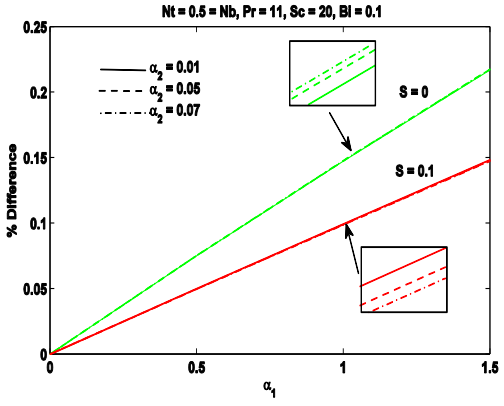

Figure 3.12 % Difference of $\boldsymbol{\alpha_1}$, $\boldsymbol{\alpha_2}$ on $-\boldsymbol{\theta'(0)}$ for $\boldsymbol{S}$

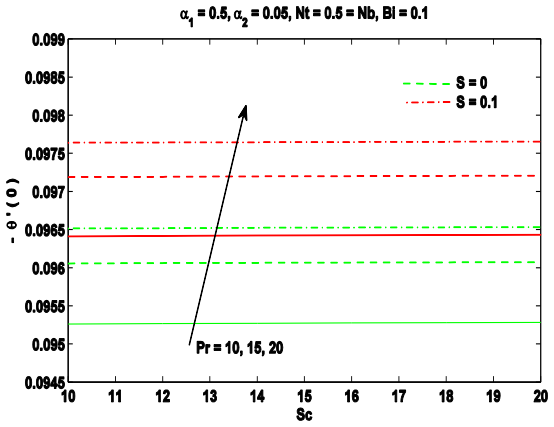

Figure 3.13 Effect of Pr, Sc on $-\theta'(0)$ for S

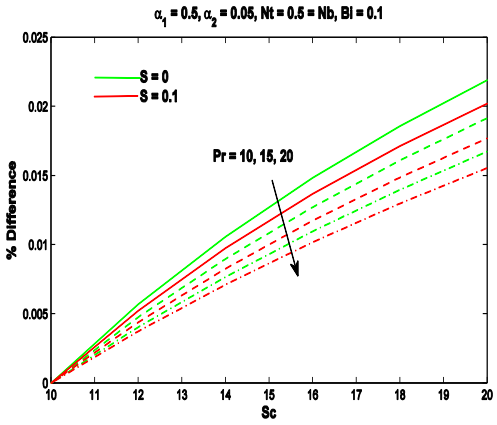

Figure 3.14 % Difference of Pr, Sc on $-\theta'(0)$ for S

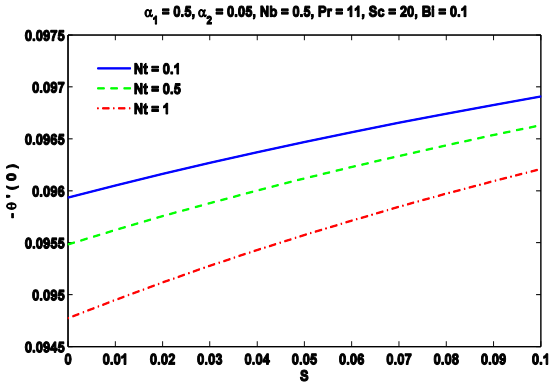

Figure 3.15 Effect of Nt on $-\theta'(0)$ for S

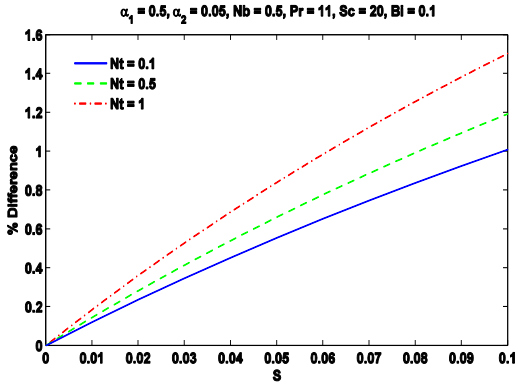

Figure 3.16 % Difference of Nt on $-\theta'(0)$ for S

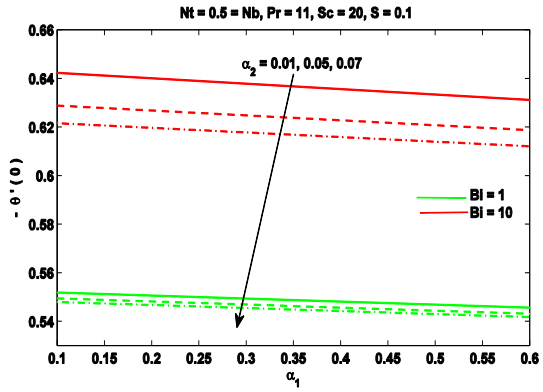

Figure 3.17 Effect of $\boldsymbol{\alpha_1}$, $\boldsymbol{\alpha_2}$ on $-\boldsymbol{\theta'(0)}$ for $\boldsymbol{Bi}$

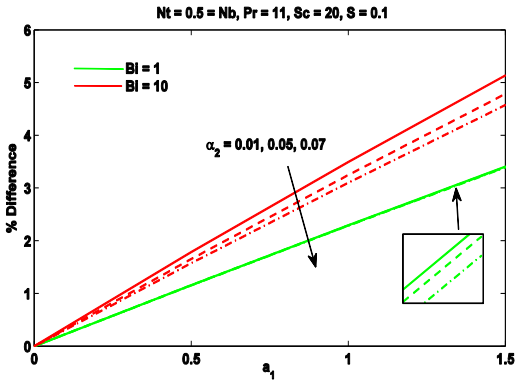

Figure 3.18 % Difference of α_1, α_2 on $-\theta'(0)$ for Bi

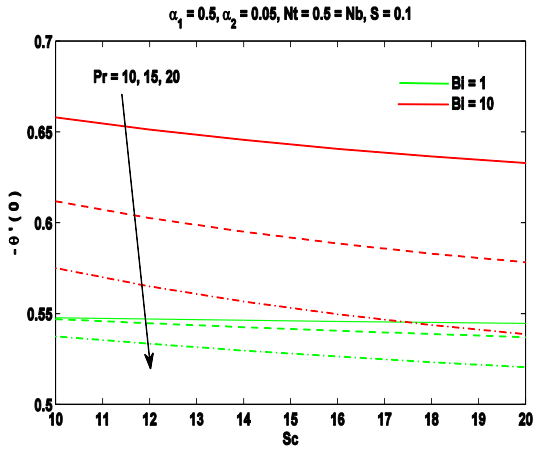

Figure 3.19 Effect of Pr, Sc on $-\theta'(0)$ for Bi

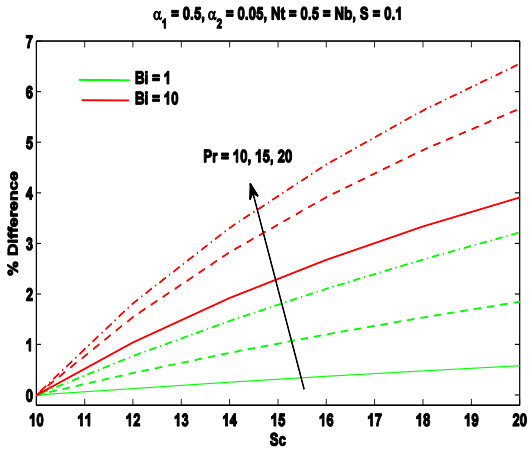

Figure 3.20 % Difference of Pr, Sc on $-\theta'(0)$ for Bi

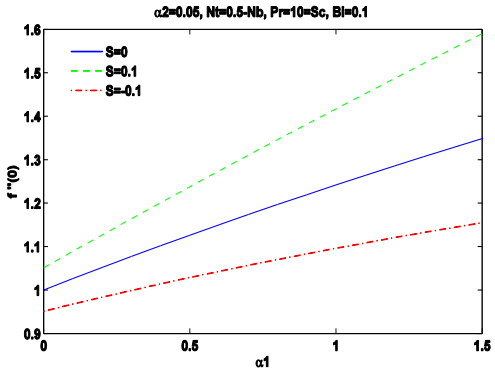

Figure 3.21 Effects of $\boldsymbol{\alpha_1}$ and S on $\boldsymbol{f''(0)}$

Table 3.1 Numerical results of reduce Nusselt number for variation of different parameters

α_1	α_2	S	Nt	Nb	Pr	Sc	Bi	$-\theta'(0)$
0.5	0.05	0.1	0.5	0.5	15	20	0.1	0.0972063
1								0.0971746
1.5								0.0971433
0.5	0.01							0.0971634
	0.05							0.0972063
	0.07							0.097227619
	0.05	0						0.0960739
		0.1						0.0972063
		0.1	0.1					0.0974718
			0.5					0.0972063
			1					0.0967914
			0.5	0.5				0.0972063
				1				0.0972063
				1.5				0.0972063
				0.5	10			0.0964325
					15			0.0972063
					20			0.0976554
					15	10		0.0971891
						15		0.0971989
						20		0.0972063
						20	1	0.537005
							10	0.0578211

Chapter 4
Simulations by revised Cattaneo Christov model

4.1 Introduction

In this chapter the basic problem is the same as in previous difference is the use of Cattaneo Christov model in association with non-homogeneous model Heat flux $\boldsymbol{q}$ in original Cattaneo Christov heat flux model is defined by the following differential equation.

$$\left(1+\lambda_2\frac{D}{Dt}\right)\boldsymbol{q}=-k\boldsymbol{\nabla}\mathrm{T} \tag{1.33}$$

However in non-homogeneous model it state that effective heat flux is the sum of conductive heat flux and heat flux due the nanoparticle diffusion as $\boldsymbol{q}=-k\nabla T+h_s j_s$ therefore we feel that it is logical to modify the above equation as follows

$$\left(1+\lambda_2\frac{D}{Dt}\right)\boldsymbol{q}=-k\boldsymbol{\nabla}\mathrm{T}+h_s j_s \tag{1.35}$$

As (1.33) is for homogeneous mixture whereas (1.35) should represent nonhomogeneous mixture. The detailed derivation is given is chapter 1.

4.2 Mathematical Modeling

Let us consider a 2-dimension, steady incompressible fluid over a stretching sheet. The sheet is moving with velocity $u=ax$ in x-direction, where a is constant. $v=-V_s$ Suction effects on surface. Maxwell model is considered for non-Newtonian fluid. Cattaneo-Christov heat flux model with nanofluid is adopted for heat transport. Let u, v is the velocity component along x-, y-axis, T denotes the temperature T_w and T_∞ are temperature at wall and ambient temperature respectively. C is concentration of nanoparticles and C_w, C_∞ are the concentration on wall and ambient concentration of nanoparticles respectively. Transportation of nanoparticles is observed by using non-homogeneous model.

By considering all the above assumptions the detailed derivation of our mathematical model is given in chapter 1 equatigon 1.9, 1.21, 1.54 and 1.59 and given below:

$$\frac{\partial u}{\partial x}+\frac{\partial v}{\partial y}=0 \tag{1.9}$$

$$u\frac{\partial u}{\partial x}+v\frac{\partial u}{\partial y}+\lambda_1\left(u^2\frac{\partial^2 u}{\partial x^2}+2uv\frac{\partial^2 u}{\partial x\partial y}+v^2\frac{\partial^2 u}{\partial y^2}\right)=\nu\left(\frac{\partial^2 u}{\partial y^2}\right) \tag{1.21}$$

$$\begin{aligned}u\frac{\partial T}{\partial x}+v\frac{\partial T}{\partial y}+\lambda_2\Bigg[&u^2\frac{\partial^2 T}{\partial x^2}+v^2\frac{\partial^2 T}{\partial y^2}+2uv\frac{\partial^2 T}{\partial x\partial y}+\left(u\frac{\partial u}{\partial x}+v\frac{\partial u}{\partial y}\right)\frac{\partial T}{\partial x}\\&+\left(u\frac{\partial v}{\partial x}+v\frac{\partial v}{\partial y}\right)\frac{\partial T}{\partial y}\\&+\frac{(\rho c_p)_s}{(\rho c_p)_f}\Bigg(D_B u\frac{\partial^2 C}{\partial y^2}\frac{\partial T}{\partial x}+D_B v\frac{\partial^2 C}{\partial y^2}\frac{\partial T}{\partial y}+\frac{D_T}{T_\infty}u\frac{\partial^2 T}{\partial y^2}\frac{\partial T}{\partial x}\\&+\frac{D_T}{T_\infty}v\frac{\partial^2 T}{\partial y^2}\frac{\partial T}{\partial y}+D_B Tu\frac{\partial^3 C}{\partial x\partial y^2}+D_B Tv\frac{\partial^3 C}{\partial y^3}+\frac{D_T}{T_\infty}Tu\frac{\partial^3 T}{\partial x\partial y^2}\\&+\frac{D_T}{T_\infty}Tv\frac{\partial^3 T}{\partial y^3}\Bigg)\Bigg]\\&=\frac{k}{(\rho c)_f}\left(\frac{\partial^2 T}{\partial y^2}\right)+\frac{(\rho c)_s}{(\rho c)_f}\left[D_B\left(\frac{\partial T}{\partial y}\frac{\partial C}{\partial y}\right)+\frac{D_T}{T_\infty}\left(\frac{\partial T}{\partial y}\right)^2\right]\end{aligned} \tag{1.54}$$

$$u\frac{\partial C}{\partial x}+v\frac{\partial C}{\partial y}=D_B\left(\frac{\partial^2 C}{\partial y^2}\right)+\frac{D_T}{T_\infty}\left(\frac{\partial^2 T}{\partial y^2}\right) \tag{1.59}$$

Where λ_1 is the fluid relaxation time, λ_2 is a thermal relaxation time, k is a thermal conductivity, ν is the kinematic viscosity. $(\rho c)_s$ is the specific heat capacity of particles, $(\rho c)_f$ is the specific heat capacity of non-Newtonian fluid, D_B is Brownian diffusion coefficient and D_T is the Thermophoretic diffusion coefficient. The above equations are the required partial differential equations with the following boundary conditions.

$$u = ax, \quad v = -V_s, \quad -k\frac{\partial T}{\partial y} = h_f(T_f - T), \quad \frac{\partial C}{\partial y} = 0 \quad at \ y = 0$$
$$u = 0, \qquad T = T_\infty, \qquad \frac{\partial T}{\partial y} = 0, \tag{4.1}$$
$$C = C_\infty, \qquad \frac{\partial C}{\partial y} = 0 \qquad at \ y \to \infty$$

First condition at $y = 0$ shows the stretchiness in sheet, second condition represents suction effect on the surface if $V_s > 0$ shows the suction velocity and $V_s < 0$ shows injection velocity, and third condition shows convective heat transfer in which k is a thermal conductivity, h_f is the convective heat transfer coefficient of fluid, T_f is fluid temperature. T_∞ represents ambient temperature and C_∞ represents ambient concentration of nanoparticles respectively. The following similarity transformation is used in the above equations in order to attain required ordinary differential equation.

$$\eta = y\sqrt{\frac{a}{\nu}}, \qquad \psi = x\sqrt{a\nu}f(\eta), \tag{2.2}$$

$$\theta(\eta) = \frac{T - T_\infty}{T_w - T_\infty}, \qquad \varphi(\eta) = \frac{C - C_\infty}{C_w - C_\infty} \tag{4.2}$$

Equation (1.9) satisfies by using these transformations and equation (1.21), (1.54) and (1.59) are converted into following ordinary differential equations.

$$(1 - \alpha_1 f^2)f''' + (1 + 2\alpha_1 f')ff'' - f'^2 = 0 \tag{4.3}$$

$$-Nt\alpha_2(T_R + \theta)f\theta''' + \left(\alpha_2 f^2 - \frac{1}{Pr} - Nt\alpha_2 f\theta'\right)\theta'' + (\alpha_2 f' - 1 - Nb\alpha_2\varphi'')f\theta' - Nb\alpha_2(T_R + \theta)f\varphi''' - Nb\varphi'\theta' - Nt(\theta')^2 = 0 \tag{4.4}$$

$$\varphi'' + \frac{Nt}{Nb}\theta'' + Scf\varphi' = 0 \tag{4.5}$$

Where $\alpha_1 = a\lambda_1$ is the relaxation parameter, Nt is Thermophoresis parameter and defines as $Nt = D_T(\rho c)_p(T_w - T_\infty)/(\rho c)_f T_\infty \nu$, $\alpha_2 = a\lambda_2$ is thermal relaxation parameter, $T_R = T_\infty/T_f - T_\infty$, Pr is a Prandtl number and define as $Pr = \nu/\alpha$, Brownian motion parameter define as $Nb = D_B(\rho c)_p(C_w - C_\infty)/(\rho c)_f \nu$ and $Sc = \nu/D_B$ is a Schmidt number. Their boundary conditions are also transformed in following form:

$$f'(0) = 1, \quad f(0) = S, \quad \theta'(0) = Bi(\theta(0) - 1), \quad \varphi'(0) = 1 \quad at \ \eta = 0$$

$$f'(\infty) = 0, \qquad \theta(\infty) = 0, \qquad \theta'(\infty) = 0, \tag{4.6}$$

$$\varphi(\infty) = 0, \qquad \varphi'(\infty) = 0 \quad at \ \eta \to \infty$$

In which $S = V_s/\sqrt{av}$ is a suction parameter and Bi is a Biot number which is defines as $Bi = \frac{k}{h}\sqrt{\frac{a}{x}}$.

The skin friction coefficient is defined as:

$$C_f = \frac{\tau_x}{\rho U^2} \tag{4.7}$$

And local Nusselt number is defined as:

$$Nu_x = \frac{xq_x}{k_f\left(T_f - T_\infty\right)} \tag{4.8}$$

In which $\tau_x = \left(-\mu_{nf}\frac{\partial u}{\partial y}\Big|_{y=0}\right)$ and $q_x = \left(-k_{nf}\frac{\partial T}{\partial y}\Big|_{y=0}\right)$ after using these, our skin friction coefficient and local Nusselt becomes as:

$$Nu_x = -\theta'(0) \tag{4.9}$$

$$C_f = f''(0) \tag{4.10}$$

.

4.3 Solution Methodology

In order to solve the above non-dimensionalized ordinary differential equations (4.3), (4.4) and (4.5) along with their boundary conditions (4.6) we will follow an implicit finite difference scheme known as Keller-box method. In first step import few new dependent variables

.

$$f' = u,\ \ u' = v,\ \ u'' = v'$$

$$\theta' = y,\ \ y' = z,\ \ y'' = z' \tag{4.11}$$

$$\varphi' = p,\ \ p' = q,\ \ \ p'' = q'$$

Insert these variables (4.11) in above equations (4.3), (4.4) and (4.5) so they transformed into first order differential equations:

$$(1 - \alpha_1 f^2)v' + (1 + 2\alpha_1 u)fv - u^2 = 0 \tag{4.12}$$

$$-Nt\alpha_2(T_R + \theta)fz' + \left(\alpha_2 f^2 - \frac{1}{Pr} - Nt\alpha_2 fy\right)z + (\alpha_2 u - 1 - Nb\alpha_2 q)fy - Nb\alpha_2(T_R + \theta)fq' - Nbpy - Nt(y)^2 = 0 \tag{4.13}$$

$$q + \frac{Nt}{Nb}z + Scfp = 0 \tag{4.14}$$

In order to gets the finite difference equation, the above equations solved by using the centered difference scheme for derivatives and averages, after that using Newton's method to linearize the non-linear system of our equations. Then these linearized difference equation write as the system of matrix vector form which is known as tridiagonal matrix form and these matrices solved by using Block-Elimination method. For this purpose use the MATLAB code with tolerance 10^{-6}.

4.4 Numerical Results and Discussion

In this section we will discuss the numerical results of nonlinear differential equation (4.12)-(4.14) which are calculated by using the Keller-box method. These results are for different parameters such as α_1 relaxation parameter, α_2 thermal relaxation parameter, S Suction parameter, Bi is Biot number, Nt is Thermophoresis parameter, Nb is Brownian motion parameter, Pr is Prandtl number, Sc is Schmidt number and T_R.

In figure 4.1 we present the effect of relaxation parameter and suction parameter on $f'(\eta)$. Increasing value of relaxation parameter and suction parameter shows the reduction in velocity boundary layer thickness. Effect of these two parameters on temperature boundary layer represents in figure 4.2, bigger value of these parameters shows the increment in thermal boundary layer. Variation of thermal relaxation parameter depicts the mix behavior towards the thermal boundary layer on the other hand increment in Biot number increase boundary layer as shown in figure 4.3. The figure 4.4 is representing the demeanor of thermophoresis parameter and browning motion parameter on thermal boundary layer. Thermophoresis parameter increases θ whereas Brownian motion parameter reduces. Prandtl number and Schmidt number performance is in figure 4.5, which is clearly seen that due to Prandtl number thermal boundary decreases and with Schmidt number thermal boundary layer reduces. Figure 4.6 showing the behavior of T_R and it depicts that increasing value of T_R thermal boundary layer also increases. Figure 4.7 – 4.11 are presenting the concentration profile of nanoparticles. Relaxation parameter leaves positive impact on concentration boundary layer but suction drags downwards concentration boundary layer profile according to figure 4.7. Thermal relaxation parameter showing the mix behavior and Biot number both is showing the decreasing profile in figure 4.8. Figure 4.9 representing the actions of Brownian motion parameter and Thermophoresis parameter on concentration boundary layer. It is clearly seen that concentration boundary layer arises with bigger values of Nt, and Nb is showing increasing behavior towards this profile. Figure 4.10 is showing the performance of Prandtl number and Schmidt number. So concentration profile showing the decreasing behavior with increasing value of Prandtl number and Schmidt number is also presenting the decreasing behavior towards it. In figure 4.11 T_R is presenting the mix demeanor towards the concentration bounder layer. Figure 4.12 is representing the skin friction coefficient attitude and it is showing the decreasing behavior with the increasing value of relaxation parameter. Figure 4.13 is showing effect of α_1 and α_2 on rate of change of surface temperature as a function of S, α_1 is showing reduction in the rate of change of surface temperature on the other hands α_2 is depicting mix behavior. Figure 4.14 representing the performance of Brownian motion parameter and Thermophoresis parameter on $-\theta'(0)$ for suction. With Nb surface heat transfer rate is increasing and Nt showing a decreasing behavior. Prandtl number and Schmidt number both are showing the positive response towards $-\theta'(0)$ in figure 4.15 Increasing T_R reduces surface heat transfer rate as shown in figure 4.16.

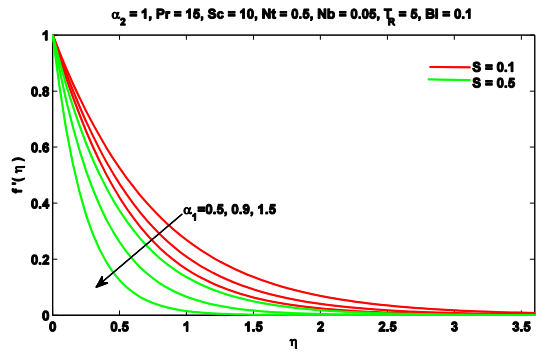

Figure 4.1 Effect of α_1 and S on $f'(\eta)$

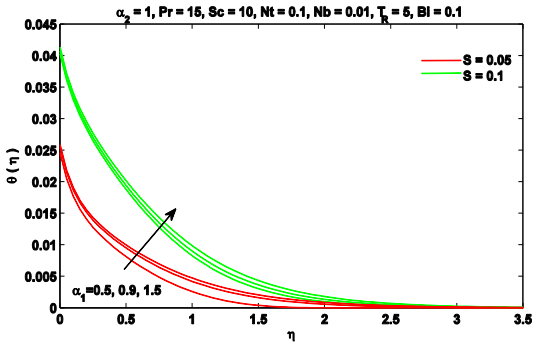

Figure 4.2 Effect of α_1 and S on θ

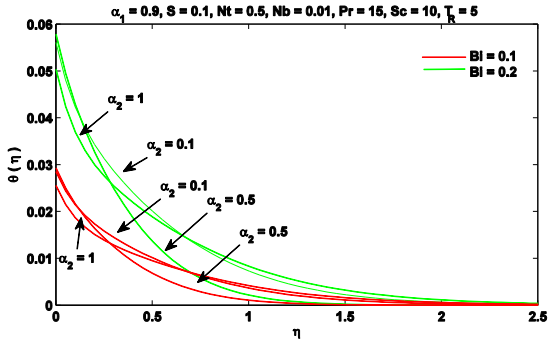

Figure 4.3 Effect of α_2 and Bi on θ

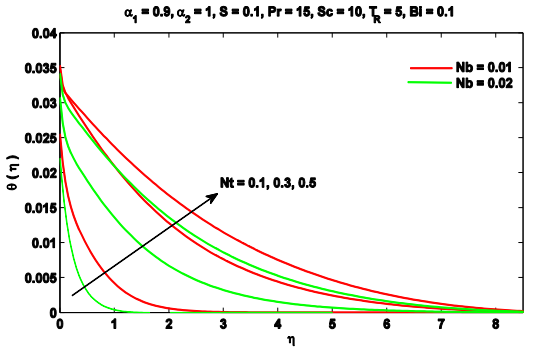

Figure 4.4 Effect of Nt and Nb on θ

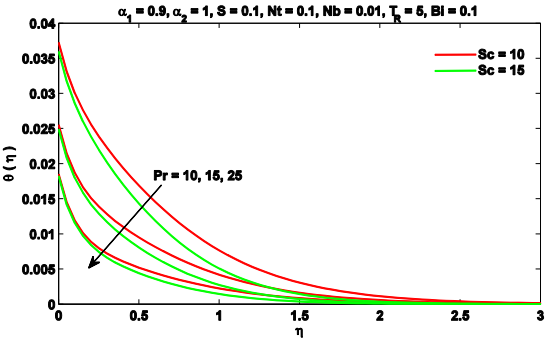

Figure 4.5 Effect of Pr and Sc on θ

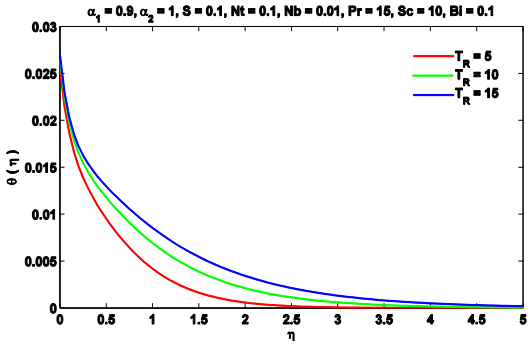

Figure 4.6 Effect of T_R on θ

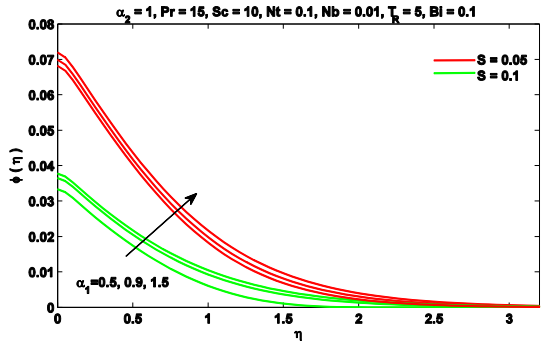

Figure 4.7 Effect of α_1 and S on φ

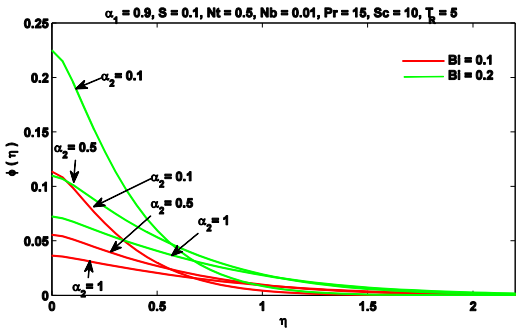

Figure 4.8 Effect of α_2 and Bi on φ

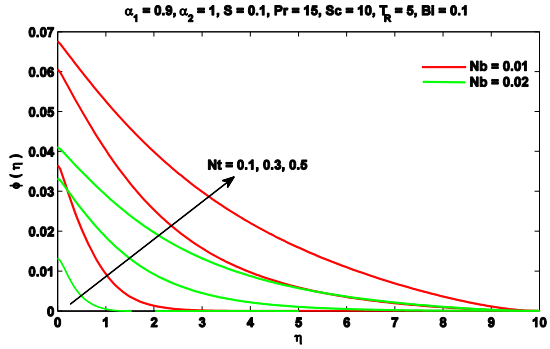

Figure 4.9 Effect of Nt and Nb on φ

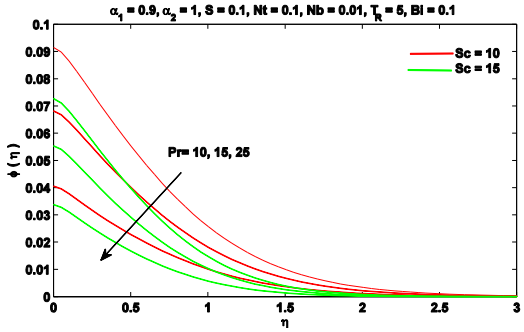

Figure 4.10 Effect of Pr and Sc on φ

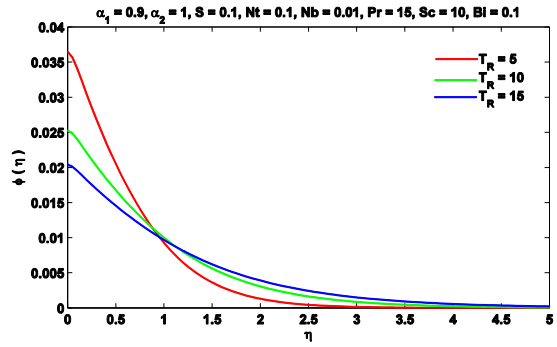

Figure 4.11 Effect of T_R on φ

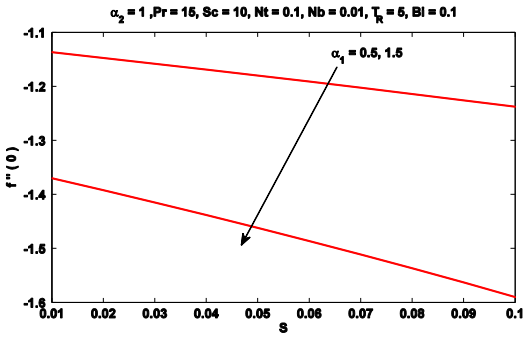

Figure 4.12 Effect of α_1 and S on skin friction coefficient

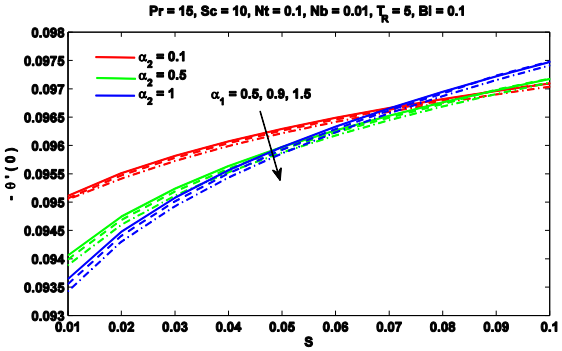

Figure 4.13 Effect of α_1 and α_2 on $-\theta'(0)$ for S

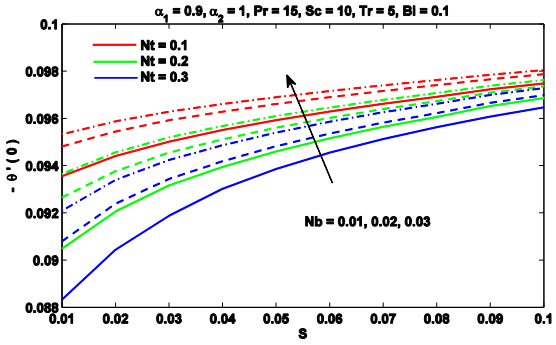

Figure 4.14 Effect of Nt and Nb on$-\theta'(0)$ for S

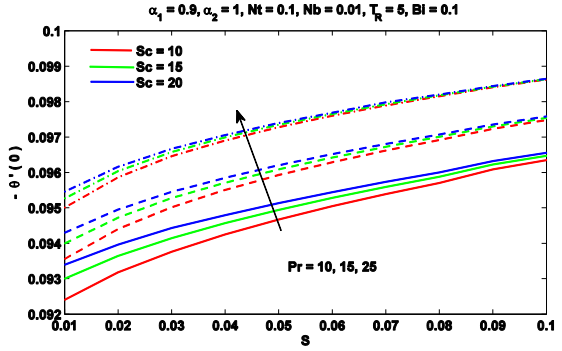

Figure 4.15 Effect of Pr and Sc on $-\theta'(0)$ for S

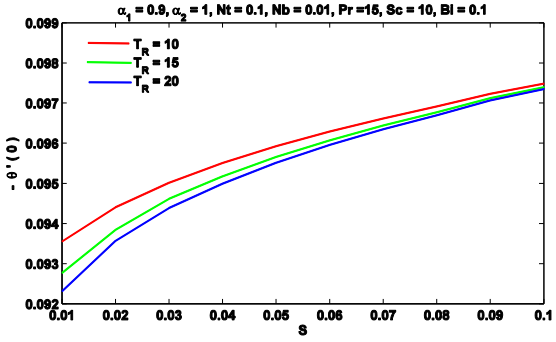

Figure 4.16 Effect of T_R on $-\theta'(0)$ for S

Table 4.1 Numerical results of reduced Nusselt number for variations of different parameters

α_1	α_2	S	Nt	Nb	Pr	Sc	Bi	T_R	$-\theta'(0)$
0.5	0.5	0.1	0.5	0.02	15	15	0.1	5	0.0962001
0.9									0.0962388
1.5									0.0961447
0.5	0.1								0.0962182
	0.5								0.0962001
	1								0.0965349
	0.5	0.05							0.0940419
		0.1							0.0962001
		0.1	0.1						0.0975514
			0.3						0.0995651
			0.5						0.101194
			0.5	0.01					0.0870721
				0.02					0.0913148
				0.03					0.093306
				0.02	10				0.094676
					15				0.0962001
					20				0.0970834
					15	10			0.0961453
						15			0.0962001
						20			0.0962568
						15	0.1		0.0962001
							0.2		0.184996
							0.1	5	0.0962001
								10	0.096131

4.5 Conclusion

In Chapter 3 and 4 we have tried to solve same problem using two different mathematical formulations. Chapter 3 formulations can be found in most of the literature available, during this study we have noticed that in available literature researchers neglected the part of heat flux due to nanoparticle diffusion which affect the governing ODEs of energy and concentration. This missing term is added in chapter 4 and re-formulates the problem. Although we have obtained the numerical results but solution show a nonrealistic and oscillatory behavior for this new problem when plotted for the same parameters. The realistic results for some particular ranges/smaller values of Brownian motion parameter are given above in fig4.2 to fig 4.6 while the nonrealistic is given in figures (b) below.

Figures from Chapter 3

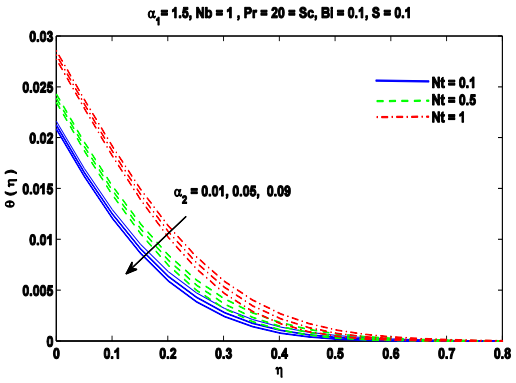

Figure 4.17a Effects of α_2 and Nt on θ

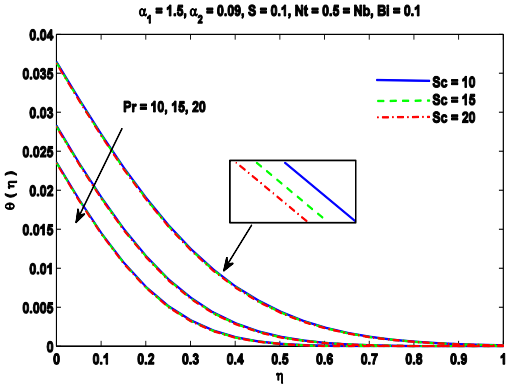

Figure 4.18a Effect of Pr and Sc on θ

Figures from Chapter 4

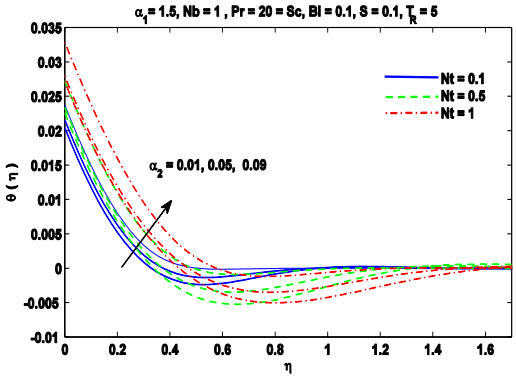

Figure 4.17b Effects of α_2 and Nt on θ

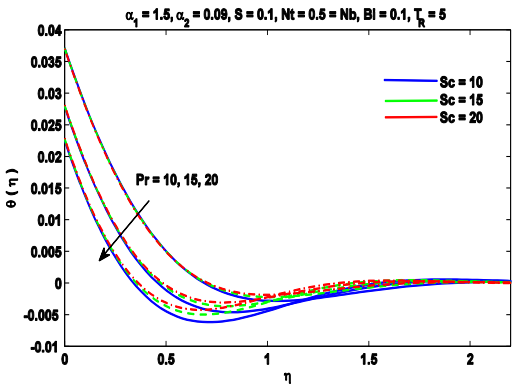

Figure 4.18b Effect of Pr and Sc on θ

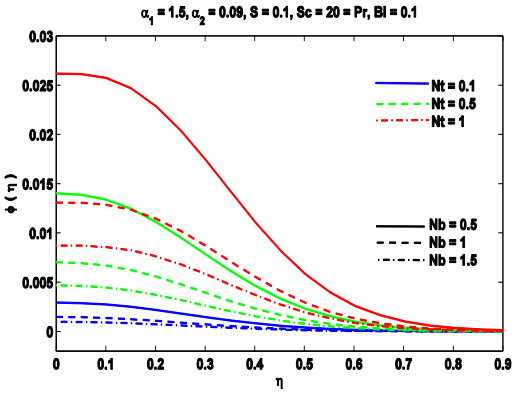

Figure 4.19a Effect of Nt, Nb on φ

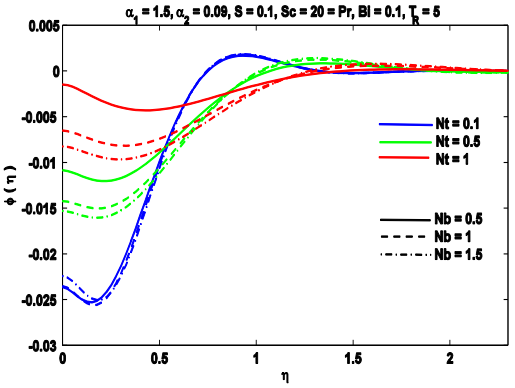

Figure 4.19b Effect of Nt, Nb on φ

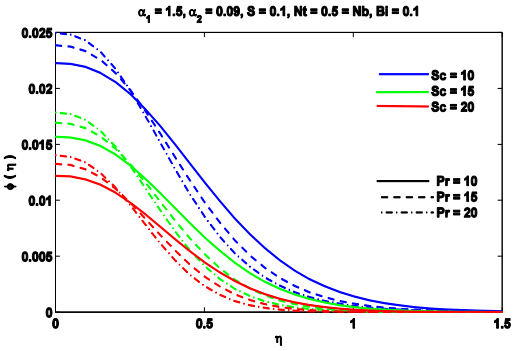

Figure 4.20a Effect of Pr and Sc on φ

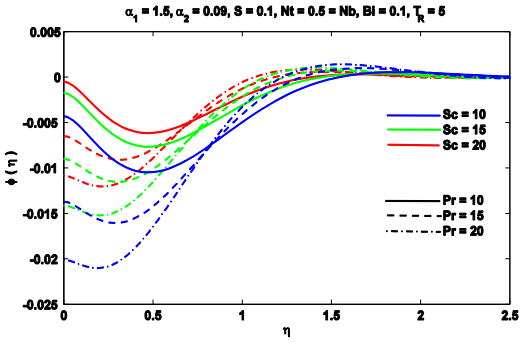

Figure 4.20b Effect of Pr and Sc on φ

Chapter 5
Conclusion and Future work

In this exposition we focused on non-Newtonian (upper convective Maxwell fluid) along with Cattaneo Christov heat flux model and obtained the numerical results through homogeneous model and non-homogeneous model. Velocity boundary layer profiles for all three problems does not affects as its mathematical model remains same for them. On the other hand temperature profiles vary problem to problem. For homogeneous model Ethanol is taken as a base fluid along with five various types of nanoparticles. It is a homogenous model and it shows increases skin friction coefficient with suction and relaxation parameter. In spite of that local Nusselt number shows opposite affects with relaxation parameter. Recently researchers has started work on hybrid model of homogeneous model, so in future we can continue our work with Hybrid model and compare the results. Non-homogenous model of calculating nanofluid behavior is Buongiorno model and it's also considers concentration profiles of nanoparticles. First we have examined the problem by using the same model, which is already presented in the literature. Relaxation parameter, thermal relaxation parameter, Prandtal number, Schmidt number all the parameters are showing positive response and Thermophoresis parameter is decreasing towards the reduced Nusselt number with suction. Reduced Nusselt number, along with relaxation parameter, thermal relaxation parameter, Prandtl number and Schmidt number is showing decreasing response for Biot number. Likewise the homogeneous model, in non-homogeneous model skin friction coefficient is showing the increasing behavior with suction. During the study of non-homogeneous model it is notified that the part of heat flux due to nanoparticle diffusion is neglected which is an important term. We have added that term in governing equation of energy and solved first problem related to revise Cattaneo Christov model. In spite of the fact we obtained the numerical solutions but the solution shows oscillatory/ unrealistic behavior for the modified model. So through this problem not only grabbed the attention of researchers but also invites them to solve more problems using this revised model.

References:

[1] J. D. Anderson, “Ludwig Prandtl’s boundary layer,” *Phys. Today*, vol. 58, no. 12, pp. 42–48, 2005.

[2] L. J. Crane, “Flow past a stretching plate,” *Zeitschrift für Angew. Math. und Phys. ZAMP*, vol. 21, no. 4, pp. 645–647, 1970.

[3] S. U. S. Choi and J. A. Eastman, “Enhancing thermal conductivity of fluids with nanoparticles,” *ASME Int. Mech. Eng. Congr. Expo.*, vol. 66, no. March, pp. 99–105, 1995.

[4] S. Mukherjee, “Preparation and Stability of Nanofluids-A Review,” *IOSR J. Mech. Civ. Eng.*, vol. 9, no. 2, pp. 63–69, 2013.

[5] J. Buongiorno, “Convective Transport in Nanofluids,” *J. Heat Transfer*, vol. 128, no. 3, p. 240, 2006.

[6] D. Y. Tzou, “Thermal instability of nanofluids in natural convection,” *Int. J. Heat Mass Transf.*, vol. 51, no. 11–12, pp. 2967–2979, 2008.

[7] A. V. Kuznetsov and D. A. Nield, “The Cheng-Minkowycz problem for natural convective boundary layer flow in a porous medium saturated by a nanofluid: A revised model,” *Int. J. Heat Mass Transf.*, vol. 65, pp. 682–685, 2013.

[8] B. Straughan, “Thermal convection with the Cattaneo-Christov model,” *Int. J. Heat Mass Transf.*, vol. 53, no. 1–3, pp. 95–98, 2010.

[9] W. A. Khan and I. Pop, “Boundary-layer flow of a nanofluid past a stretching sheet,” *Int. J. Heat Mass Transf.*, vol. 53, no. 11–12, pp. 2477–2483, 2010.

[10] A. V. Kuznetsov and D. A. Nield, “Natural convective boundary-layer flow of a nanofluid past a vertical plate,” *Int. J. Therm. Sci.*, vol. 49, no. 2, pp. 243–247, 2010.

[11] R. C. Bataller, “Numerical Comparisons of Blasius and Sakiadis Flows,” *Malaysian J.*

Ind. Appl. Math., vol. 26, no. 2, pp. 187–196, 2010.

[12] O. D. Makinde and A. Aziz, "Boundary layer flow of a nanofluid past a stretching sheet with a convective boundary condition," *Int. J. Therm. Sci.*, vol. 50, no. 7, pp. 1326–1332, 2011.

[13] M. Hatami, M. Sheikholeslami, and D. D. Ganji, "Laminar fl ow and heat transfer of nano fl uid between contracting and rotating disks by least square method," *Powder Technol.*, vol. 253, pp. 769–779, 2014.

[14] M. Mustafa, J. A. Khan, T. Hayat, and A. Alsaedi, "On Bödewadt flow and heat transfer of nanofluids over a stretching stationary disk," *J. Mol. Liq.*, vol. 211, pp. 119–125, 2015.

[15] N. A. Abu Bakar, N. Bachok, and N. M. Arifin, "Boundary layer flow and heat transfer in nanofluid over a stretching sheet using Buongiorno model and thermophysical properties of nanoliquids," *Indian J. Sci. Technol.*, vol. 9, no. 31, pp. 1–9, 2016.

[16] J. A. Khan, M. Mustafa, T. Hayat, and A. Alsaedi, "Numerical study of cattaneo-christov heat flux model for viscoelastic flow due to an exponentially stretching surface," *PLoS One*, vol. 10, no. 9, pp. 1–10, 2015.

[17] M. E. Ali and N. Sandeep, "Cattaneo-Christov model for radiative heat transfer of magnetohydrodynamic Casson-ferrofluid: A numerical study," *Results Phys.*, vol. 7, pp. 21–30, 2017.

[18] F. M. Abbasi and S. A. Shehzad, "Heat transfer analysis for three-dimensional flow of Maxwell fluid with temperature dependent thermal conductivity: Application of Cattaneo-Christov heat flux model," *J. Mol. Liq.*, vol. 220, pp. 848–854, 2016.

[19] M. Mustafa, T. Hayat, and A. Alsaedi, "Rotating flow of Maxwell fluid with variable thermal conductivity: An application to non-Fourier heat flux theory," *Int. J. Heat Mass Transf.*, vol. 106, pp. 142–148, 2017.

[20] K. Rubab and M. Mustafa, "Cattaneo-Christov heat flux model for MHD three-dimensional flow of Maxwell fluid over a stretching sheet," *PLoS One*, vol. 11, no. 4, pp. 1–16, 2016.

[21] T. Muhammad, A. Alsaedi, S. A. Shehzad, and T. Hayat, “A revised model for Darcy-Forchheimer flow of Maxwell nanofluid subject to convective boundary condition,” *Chinese J. Phys.*, vol. 55, no. 3, pp. 963–976, 2017.

[22] M. I. Khan, M. Ijaz Khan, M. Waqas, T. Hayat, and A. Alsaedi, “Chemically reactive flow of Maxwell liquid due to variable thicked surface,” *Int. Commun. Heat Mass Transf.*, vol. 86, no. June, pp. 231–238, 2017.

[23] A. Shahid, M. M. Bhatti, O. A. Bég, and A. Kadir, “Numerical study of radiative Maxwell viscoelastic magnetized flow from a stretching permeable sheet with the Cattaneo–Christov heat flux model,” *Neural Comput. Appl.*, vol. 30, no. 11, pp. 3467–3478, 2018.

[24] A. Rahimi Gheynani *et al.*, “Investigating the effect of nanoparticles diameter on turbulent flow and heat transfer properties of non-Newtonian carboxymethyl cellulose/CuO fluid in a microtube,” *Int. J. Numer. Methods Heat Fluid Flow*, vol. 29, no. 5, pp. 1699–1723, 2019.

[25] M. Amani, P. Amani, M. Bahiraei, and S. Wongwises, “Prediction of hydrothermal behavior of a non-Newtonian nanofluid in a square channel by modeling of thermophysical properties using neural network,” *J. Therm. Anal. Calorim.*, vol. 135, no. 2, pp. 901–910, 2019.

[26] M. Goodarzi, “Slip velocity and temperature jump of a non-Newtonian nano fl uid , aqueous solution of carboxy-methyl cellulose / aluminum oxide nanoparticles , through a microtube,” *Int. J. Numer. Methods Heat Fluid Flow*, vol. 29, no. 5, pp. 1606–1628, 2018.

[27] H. Maleki and M. Reza, “Flow and heat transfer in non-Newtonian nanofluids over porous surfaces,” *J. Therm. Anal. Calorim.*, vol. 135, no. 3, pp. 1655–1666, 2019.

[28] Z. Wu and R. Zhang, “Learning physics by data for the motion of a sphere falling in a non-Newtonian fluid,” *Commun. Nonlinear Sci. Numer. Simul.*, vol. 67, pp. 577–593, 2019.

[29] J. Alebraheem, “Flow of nanofluid with Cattaneo – Christov heat flux model,” *Appl. Nanosci.*,vol. 35, no. 7, pp. 756, 2019.

[30] A. Saadatmandi, “Sinc-collocation method for solving sodium alginate (SA)

non-Newtonian nanofluid flow between two vertical flat plate," *J. Brazilian Soc. Mech. Sci. Eng.*, vol. 41, p. 158, 2019.

[31] K. Parand, "A rational approximation to the boundary layer flow of a non-Newtonian fluid," *J. Brazilian Soc. Mech. Sci. Eng.*, vol. 41, p. 125, 2018.

[32] I. Pishkar, B. Ghasemi, A. Raisi, and S. M. Aminossadati, "Numerical study of unsteady natural convection heat transfer of Newtonian and non-Newtonian fluids in a square enclosure under oscillating heat flux," *J. Therm. Anal. Calorim.*, vol. 1, no. m, 2019.

[33] G. Sarojamma, R. V. Lakshmi, P. V. S. Narayana, and I. L. Animasaun, "Exploration of the Significance of Autocatalytic Chemical Reaction and Cattaneo-Christov Heat Flux on the Dynamics of a Micropolar Fluid," *J. Appl. Comput. Mech.*, vol. 6, no. 1, pp. 77–89, 2020.

[34] R. K. Tiwari and M. K. Das, "Heat transfer augmentation in a two-sided lid-driven differentially heated square cavity utilizing nanofluids," *Int. J. Heat Mass Transf.*, vol. 50, no. 2007, pp. 2002–2018, 2018.

[35] J. Buongiorno, "Convective Transport in Nanofluids," *J. Heat Transfer*, vol. 128, no. 3, p. 240, 2006.

[36] C. I. Christov, "On frame indifferent formulation of the Maxwell – Cattaneo model of finite-speed heat conduction," *Mech. Res. Commun.*, vol. 36, no. 4, pp. 481–486, 2009.

[37] M. Z. Salleh, "Mathematical Model For The Boundary Layer Flow Due To A Moving Flat Plate," University Teknologo Malaysia, 2014. (Phd. Thesis)

[38] M. S. Abel, J. V Tawade, and M. M. Nandeppanavar, "MHD flow and heat transfer for the upper-convected Maxwell fluid over a stretching sheet," *Springer Link*, vol. 47, no. 2, pp. 385–393, 2012.

[39] A. M. Megahed, "Variable fluid properties and variable heat flux effects on the flow and heat transfer in a non- Newtonian Maxwell fluid over an unsteady stretching sheet with slip velocity Variable fluid properties and variable heat flux effects on the flow and heat tra," *Chinese Phys. B*, vol. 22, no. 9, p. 094701, 2013.

[40] K. Sadeghy, H. Hajibeygi, and S. Taghavi, “Stagnation-point flow of upper-convected Maxwell fluids,” *Int. J. Non. Linear. Mech.*, vol. 41, pp. 1242–1247, 2006.

```
function Draft_bvp4c
% F    F'    G    G'    H     T     T'
% f(1) f(2)  f(3) f(4)  f(5)  f(6)  f(7)
% clc
% clear all
L        = 10;

ls       = {'-' '--' '-.' ':'};
lc       = {'r' 'g' 'b' 'k' 'y' 'c' 'm'};
```

```
% p = [0 0.05 0.1 0.2];
%% solution



a1=1.4;
a2=0.09;
S1=0.2;
Pr=11;
Nb=0.05;
Nt=0.5;
NtNb = Nt/Nb;
Sc=20;
r=0.1;


sol = bvpinit(linspace(0,L, 10), [0 0 0 0 0 0 0]);% [1 0 0 0 0])
linspace(0,6, 25) first value and other on linspace(0, 5, 25)
for f and linspace(0,6, 25) for theta
sol1 = bvp5c(@bvp3D, @bc3D, sol);
xsol = linspace(0,L, 200);
ysol = deval(sol1,xsol);

ysol(:, 1)
plot(xsol, ysol(2, :),'LineStyle',ls{1},'Color',lc{1})
hold on
% plot(xsol, ysol(4, :),'LineStyle',ls{1},'Color',lc{2})
% hold on
% plot(xsol, ysol(6, :),'LineStyle',ls{1},'Color',lc{3})
% hold on

% F    F'    F''    T(0)   T'(0)    P(0)    P'(0)
% f(1) f(2)  f(3)   f(4)    f(5)    f(6)     f(7)
    function res = bc3D(f0, finf)

        res  = [f0(1)-S1; f0(2)-1; finf(2); f0(5)+r*(1-f0(4));
finf(4); f0(7); finf(6)];
```

```
    end

    function fvec = bvp3D(t,f)

        ff1     =  (f (2)^2 -f(1)*f(3) -
2*a1*f(1)*f(2)*f(3))/(1-a1*f (1)^2);
        ff2     =  (a2*f(1)*f(2)*f(5) - f(1)*f(5) - Nt*f (5)^2 -
Nb*f(5)*f(7))/((1/Pr) -a2*f (1)^2);
        ff3     =  -(NtNb*ff2 +Sc*f(1)*f(7));
        fvec  = [f(2); f(3); ff1; f(5); ff2; f(7); ff3];
        %         here only give derivatives with oder
    end

end
```

```
function Draft_bvp4c
% F    F'    G    G'    H     T     T'
% f(1) f(2)  f(3) f(4)  f(5)  f(6)  f(7)
clc
% clear all
L        =5;

ls       = {'-' '--' '-.' ':'};
lc       = {'r' 'g' 'b' 'k' 'y' 'c' 'm'};
```

```
% p = [0 0.05 0.1 0.2];
%% solution



        a1=0.5;
        a2=0.09;
        S1=0.05;
        Pr=11;
        Nt=0.5;
        Nb=0.05;
        Tr=5;
        NtNb = Nt/Nb;
        Sc=20;
        r=.1;

sol = bvpinit(linspace(0,L, 10), [S1 0 0 0 0 0 0 0 0]);% [1 0 0
0 0]) linspace(0,6, 25) first value and other on linspace(0, 5,
25) for f and linspace(0,6, 25) for theta
sol1 = bvp4c(@bvp3D, @bc3D, sol);
xsol = linspace(0,L, 200);
ysol = deval(sol1,xsol);

ysol(:, 1)
plot(xsol, ysol(2, :),'LineStyle',ls{1},'Color',lc{1})
 hold on
% plot(xsol, ysol(4, :),'LineStyle',ls{1},'Color',lc{2})
% hold on
% plot(xsol, ysol(7, :),'LineStyle',ls{1},'Color',lc{3})
% hold on

% F    F'    F''    T(0)   T'(0)    T''(0)    P(0)    P'(0)
P'''(0)
% f(1) f(2)  f(3)   f(4)    f(5)    f(6)     f(7)     f(8)
f(9)
    function res = bc3D(f0, finf)
```

```
        res  = [f0(1)-S1; f0(2)-1; finf(2); finf(4); f0(5)+r*(1-
f0(4)); finf(5); finf(7); f0(8); finf(8)];
         % res  = [f0(1)-S1; f0(2)-1; finf(2); finf(4);
f0(5)+r*(1-f0(4)); finf(5); finf(7); f0(8)+NtNb*f0(5); finf(8)];
    end

    function fvec = bvp3D(t,f)

        ff1     =  (f (2)^2 -f(1)*f(3) -
2*a1*f(1)*f(2)*f(3))/(1-a1*f (1)^2);
        ff2     =  -(NtNb*f(6) +Sc*f(1)*f(8));
        ff3     =  (a2*f(6)*f (1)^2-Nt*a2*f(1)*f(5)*f(6)-
(1/Pr)*f(6)+a2*f(1)*f(2)*f(5)-f(1)*f(5)-Nb*a2*f(1)*f(5)*ff2-
Nb*f(8)*f(5)-Nt*f (5)^2-
Nb*a2*(Tr+f(4))*f(1)*f(9))/(Nt*a2*(Tr+f(4))*f(1));

        fvec  = [f(2); f(3); ff1; f(5); f(6); ff2; f(8); ff3;
f(9)];
        %         here only give derivatives with oder
    end

end
```

```
function Draft_bvp4c
% F    F'    F''     T(0)   T'(0)
% f(1) f(2)  f(3)    f(4)    f(5)
clc
clear all
L        = 5;

ls       = {'-' '--' '-.' ':'};
lc       = {'r' 'g' 'b' 'k' 'y' 'c' 'm'};
```

```
p = [0 0.05 0.1 0.2];
  %% solution
  %                       rows    cps    ks
  % Copper (Cu)           8933    385    401
  % Copper oxide (CuO)    6320    531.8  76.5
  % Silver (Ag)           10500   235    429
  % Alumina (Al2O3)       3970    765    40
  % Titanium Oxide(TiO2)  4250    686.2  8.9538

         a1=0.5;
         a2=0.05;
         S1=0.2;
         rows= 6320;
         rowf=789;
         cps= 531.8;
         cpf=2840;
         ks= 76.5;
         kf=0.169;
         phi=0.1;

         Pr=18.05;
         r=10;
         cf= 1/((1-phi+(phi*(rows/rowf)))*(1-phi)^2.5);
         k=((ks+2*kf)-2*phi*(kf-ks))/((ks+2*kf)+phi*(kf-ks));
         V=(1-phi+phi*(rows*cps)/(rowf*cpf));
         ct=(1/Pr)*(k/V);




          sol = bvpinit(linspace(0,L, 10), [0.4 1 -1.36 0.52 -
4.72]);% [1 0 0 0 0]) linspace(0,6, 25) first value and other on
linspace(0, 5, 25) for f and linspace(0,6, 25) for theta
        sol1 = bvp5c(@bvp3D, @bc3D, sol);
        xsol = linspace(0,L, 200);
        ysol = deval(sol1,xsol);
```

```
%         plot(xsol, ysol(1, :),'LineStyle',ls{1},'Color',lc{1})
%         hold on
%          plot(xsol, ysol(2,
:),'LineStyle',ls{1},'Color',lc{1})
%         hold on
        plot(xsol, ysol(4, :),'LineStyle',ls{2},'Color',lc{2})
        hold on
%         plot(xsol, ysol(4, :),'LineStyle',ls{3},'Color',lc{3})
%         hold on

ysol(:, 1)

%  ysol(3,1)

% F    F'    F''    F'''(0)    T(0)   T'(0)    T''(0)
% f(1) f(2)  f(3)   ff1       f(4)    f(5)    ff2
    function res = bc3D(f0, finf)

        res  = [f0(1)-S1; f0(2)-1; finf(2); finf(4); f0(5)+r*(1-
f0(4))];
    end

    function fvec = bvp3D(t,f)

        ff1     = (f (2)^2 -f(1)*f(3) -
2*a1*f(1)*f(2)*f(3))/(cf-a1*f (1)^2);
        ff2     = -(1-a2*f(2))*f(1)*f (5)/(ct-a2*f (1)^2);

        fvec  = [f(2);f(3);ff1;f(5);ff2];
%         here only give derivatives with oder
    end

end
```